Imaging of alkyne-functionalized ruthenium complexes for photoactivated chemotherapy

Busemann, A.

APPENDIX I: GENERAL EXPERIMENTAL PROCEDURES

AI.1 Photosubstitution quantum yield measurements

The photosubstitution quantum yield can be calculated in different ways, either *via* irradiation close to an isosbestic point,[1] or *via* irradiation at a wavelength that is not an isosbestic point provided the molar extinction coefficient of the photoreaction product is known.[2] In this work, both cases were not valid and therefore, the time-dependent evolution of the UV-vis spectra were fitted using the Glotaran software package.[3] The global fitted absorption spectra of the starting material and the photoproduct allow for the calculation of their molar absorption coefficients. The time evolution of the relative concentrations of the two species was also modelled. From the time evolution of the relative concentrations and the molar absorption coefficient of all species, the time evolution of n_R and n_P, as well as $Q_{i,R}$, the total number of mol of photons absorbed between t_0 and t_i by the starting material, could be derived. The slope of the plot of n_R *vs.* $Q_{i,R}$ gives the quantum yield of the reaction.

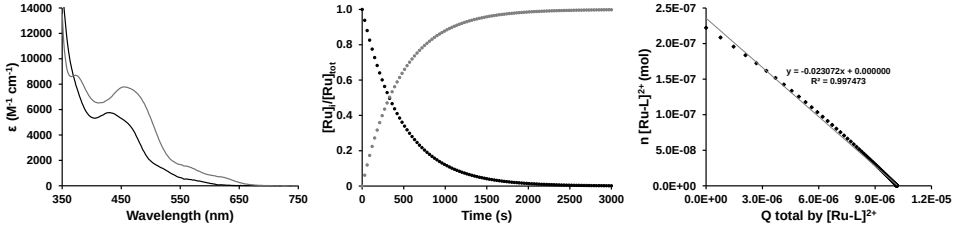

Figure AI.1. Example of the Glotaran global fitting of a one-step photosubstitution, here for the time evolution of the absorbance's of $[Ru(HCC\text{-}tpy)(i\text{-}biq)(Hmte)](PF_6)_2$ in H_2O under air atmosphere. a) Globally fitted absorption spectra of the starting material $[Ru(HCC\text{-}tpy)(i\text{-}biq)(Hmte)](PF_6)_2$ (black) and its aqua product $[Ru(HCC\text{-}tpy)(i\text{-}biq)(OH_2)]^{2+}$ (grey). b) Modelled evolution of the relative concentration of $[Ru(HCC\text{-}tpy)(i\text{-}biq)(Hmte)]^{2+}$ vs. irradiation time according to global fitting using Glotaran. c) Plot of the amount of $[Ru(HCC\text{-}tpy)(i\text{-}biq)(Hmte)]^{2+}$ (mol) vs. total amount of photons absorbed by $[Ru(HCC\text{-}tpy)(i\text{-}biq)(Hmte)]^{2+}$ (mol). The slope of the obtained line is the opposite of the quantum yield of the formation of the aqua complex. Conditions: 0.074 mM solution of $[Ru(HCC\text{-}tpy)(i\text{-}biq)(Hmte)](PF_6)_2$ in H_2O irradiated at 298 K under air atmosphere using a 517 nm LED at $5.43 \cdot 10^{-8}$ mol · s^{-1}.

AI.2 Singlet Oxygen quantum yield measurement

The quantum yield of singlet oxygen generation was determined in a custom-built setup (shown in Figure I.2), in which both UV-vis absorption and infrared emission spectroscopy could be performed. All optical parts were connected with optical fibers from Avantes (Apeldoorn, The Netherlands), with a diameter of 200-600 μm. For each measurement, 500 μL of sample, consisting of the compound in deuterated methanol ($A_{450} \leq 0.1$ for 4.0 mm pathlength), was placed in a stirred 104F-OS semi-micro fluorescence cuvette (Hellma Analytics, Müllheim, Germany) in a CUV-UV/VIS-TC temperature-controlled cuvette holder from Avantes. The sample was allowed to equilibrate at 293 K for 5 min. Emission spectroscopy

was performed with a 450 nm fiber-coupled laser (Laser system LRD-0450; Laserglow, Toronto, Canada), at 50 mW optical power (4 mm beam diameter; 0.4 W · cm^{-2}) at a 90° angle with respect to the spectrometer. The excitation power was measured using a S310C thermal sensor connected to a PM100USB power meter (Thorlabs, Dachau, Germany). Infrared emission spectra were measured from 1000 nm to 1400 nm using an Avantes NIR256-1.7TEC spectrometer, The infrared emission spectrum was acquired within 9 s, after which the laser was turned off directly. UV-vis absorption spectra before and after emission spectroscopy were measured using an Avalight-DHc halogen-deuterium lamp (Avantes) as light source (turned off during emission spectroscopy) and an Avantes 2048L StarLine UV-vis spectrometer as detector, both connected to the cuvette holder at a 180° angle. No difference in UV-vis absorption spectrum was found due to exposure to the blue laser, showing that the singlet oxygen emission is that of the starting compound. All spectra were recorded with Avasoft 8.5 software from Avantes and further processed with Microsoft Office Excel 2010 and Origin Pro 9.1 software.

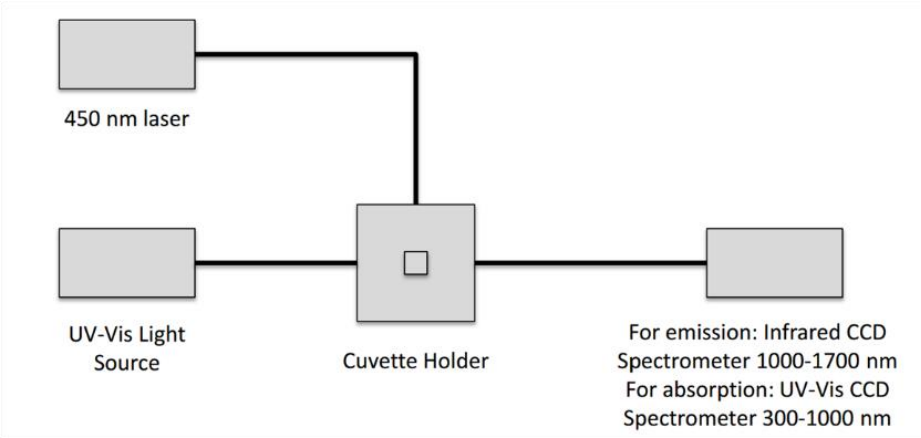

Figure AI.2. Setup for $^1O_2$ quantum yield measurement.

The quantum yield of singlet oxygen production was calculated using the relative method with $[Ru(bpy)_3]Cl_2$ as the standard (Φ_Δ = 0.73 in methanol-d_4),[4] according to:

$$\Phi_{\Delta,sam} = \Phi_{\Delta,std} \times \frac{A_{450,std}}{A_{450,sam}} \times \frac{E_{sam}}{E_{std}} \qquad \text{Equation AI.1.}$$

where Φ_Δ is the quantum yield of singlet oxygen generation, A_{450} is the absorbance at 450 nm, E is the integrated emission peak of singlet oxygen at 1274 nm, and *sam* and *std* denote the sample and standard, respectively.

AI.3 Cell culture and EC50 (photo)cytotoxicity studies

Materials

Human cancer cell line A549 (human lung carcinoma) and A431 (human epidormoid carcinoma) were distributed by the European Collection of Cell Cultures (ECACC) and purchased from Sigma Aldrich. Dulbecco's Modified Eagle Medium (DMEM, without phenol red, without glutamine), Glutamine-S (GM; 200 mM), trichloroacetic acid (TCA), glacial acetic acid, sulforhodamine B (SRB), and tris(hydroxylmethyl)aminomethane (Trisbase) were purchased from Sigma Aldrich. Fetal calf serum (FCS) was purchased from Hyclone. Penicillin and streptomycin were purchased from Duchefa and were diluted to a 100 mg/mL penicillin/streptomycin solution (P/S). Trypsin and OptiMEM (without phenol red) were purchased from Gibco Life Technologies. Trypan blue (0.4% in 0.81% sodium chloride and 0.06% potassium phosphate dibasic solution) was purchased from BioRad. Plastic disposable flasks and 96-well plates for cytotoxicity assays were purchased from Sarstedt. Cells were counted by using a BioRad TC10 automated cell counter with Biorad cell-counting slides. Cells were inspected with an Olympus IX81 microscope. UV-vis measurements for analysis of 96-well plates were performed with a M1000 Tecan Reader.

Cell Culturing

Cells were cultured in Dulbecco's Modified Eagle Medium containing phenol red, supplemented with 9.0% v/v FCS, 0.2% v/v P/S and 0.9% v/v GM (called DMEM complete) and incubated at 37 ºC at 7.0% CO_2 in 75 cm^2 T-flasks. Fresh cells were passaged at least twice after being thawed and splitted once a week at 80-90% confluency. Cells were cultured for a maxium of 8 weeks for all biological experiment.

(Photo)cytotoxicity assays

For each photocytotoxicity experiment, a parallel control plate was prepared and treated identically, but without irradiation. A549 and A431 cells were seeded at t = 0 in 96-well plates at a density of 5000 and 8000 cells/well (100 μL), respectively in OptiMEM supplemented with 2.4% v/v FCS, 0.2% v/v P/S, and 1.0% v/v GM (called OptiMEM complete) and incubated for 24 h at 37 ºC and 7.0% CO_2. Only the inner 60 wells were used for seeding, the outer wells were kept cell free to prevent border effects during irradiation. At t = 24 h, aliquots (100 μL) of six different concentrations of freshly prepared stock solutions of the compounds in OptiMEM complete were added to the wells in triplicate (see plate design in Figure I.3) and incubated for 24 h. Sterilized dimethylsulfoxide (DMSO) was used to dissolve the compounds in such amounts that the maximum v/v% of DMSO per well did not exceed 0.5%. At t = 48 h, the plates were irradiated with the cell-irradiation setup (520 nm, 30 min, 38 J/cm^2) and the control plate was kept in the dark. After irradiation, all the plates were incubated in the dark until a total time of t = 96 h after seeding. The cells were fixated by adding cold TCA (10% w/v; 100 μL) in each well and the plates were stored at 4 ºC for at least 4 h as part of the SRB assay that was adapted from Vichai *et al*.[5] In short, after fixation, the TCA medium mixture was removed from the wells, rinsed with demineralized water three times. Then, each well was stained with 100 μL SRB (0.6% w/v in 1% v/v acetic acid) for 30 min, the SRB was removed by washing with acetic acid (1% v/v), and air dried. The SRB dye was solubilized with Tris base (10 mM; 200 μL) overnight, and the absorbance in each well was read at λ = 510 nm.

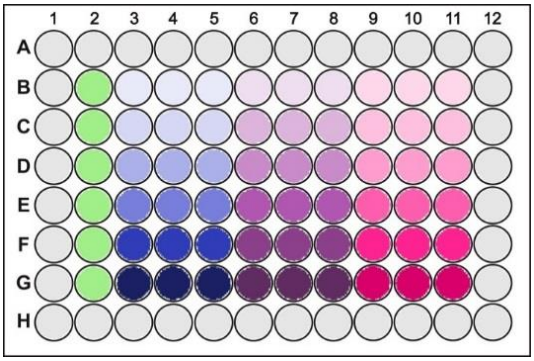

Figure AI.3. Design of a 96-well plate used in the (photo)cytotoxicity assays. Grey: Outer wells are not used for seeding to prevent border effects; green: non-treated cells (n_t = 6); blue: cells treated with compound A; purple: cells treated with compound B; pink: cells treated with compound C. Each compound was added in six different concentrations (one per row) per triplicate (n_t = 3).

The SRB absorbance data per compound per concentration was averaged over three identical wells (technical replicates, n_t = 3) in Excel and was exported to GraphPad Prism. Relative cell populations were calculated by dividing the average absorbance of the treated wells by the average absorbance of the untreated wells. It was checked that the cell viability of the untreated cells of the samples irradiated were similar (maximum difference of 10%) to the non-irradiated samples to make sure no harm was done by light alone. The resulting dose-response curve for each compound under dark and irradiated conditions was fitted to a non-linear regression function with fixed *y* maximum (100%) and minimum (0%) (relative cell viability) and a variable Hill slope. The data of three independent biological replications was used to obtain the effective concentrations (EC_{50} in μM). Photo indices (PI) were calculated, for each compound, by dividing the EC_{50} value obtained in the dark by the EC_{50} value determined under light irradiation.

AI.4 Green light irradiation in the cell irradiation setup

Cell-irradiation setup

The cell-irradiation system consisted of a Ditabis thermostat (980923001) fitted with two flat-bottomed micro-plate thermoblocks (800010600) and a 96-LED array fitted to a standard 96-well plate. The 520 nm LED (OVL-3324), fans (40 mm, 24 VDC, 9714839), and power supply (EA-PS 2042-06B) were obtained from Farnell. See Hopkins *et al.* for a full description.[6]

Determination of irradiation times

To determine which light dose is necessary to fully activate the complexes during the cytotoxicity assay, the photochemical reactivity of the ruthenium-based complexes was tested. Therefore, the inner 60 wells of a 96-well plate were filled with OptiMEM complete (100 μL, seeding without cells), and aliquots of the complexes (at their highest concentration used in the cytotoxicity assay, 250 μM) were added to the first column. The plate was irradiated for a certain amount of time, hereafter a new column was filled, and the plate was irradiated again. This process was repeated several times (irradiation times: 15, 15, 5, 5, and 5 min), and was finished with the last column filled but not irradiated. In this way, the columns were irradiated cumulative for a total time of 0, 5, 10, 15, 30, and 45 min, respectively. The absorbance of each well was measured (between 350 and 700 nm) by a M1000Tecan Reader, and corrected for the absorbance

of OptiMEM complete. The data was analyzed using Excel and the absorbance as function of time was plotted to check the time necessary for full activation (shown in Figure AIII.6).

AI.5 Cellular uptake

Cell uptake studies for the ruthenium-based complexes were conducted on A549 cancer cells at 37 °C and 21% O_2. Per compound, $1.6 \cdot 10^6$ cells were seeded in 10 mL OptiMEM complete in a 75 cm^2 flask at t = 0 h. At t = 24 h, the media was aspirated and the cells were treated with solutions of the complexes in 12 mL OptiMEM complete at a concentration of 30 μM. Treatment at the same concentration for all complexes allows for comparison of the amount of ruthenium taken up by the cells. 30 μM correlates to the lowest EC_{50} value of all complexes in the dark (EC_{50} value of [Ru(HCC-tpy)(i-Hdiqa)(Hmte)]$(PF_6)_2$). At t = 48 h, the medium was aspirated and the cells were washed twice with PBS (5 mL). The cells were trypsinized (2 mL, 5 min), suspended in OptiMEM complete (8 mL), and centrifuged (4 min, 1200 rpm). The supernatant was removed, the cells were resuspended in PBS (1 mL), and the cell count determined. The cells were centrifuged for a second time (4 min, 1200 rpm), the supernatant was aspirated, and the cell pellet stored at -80 °C.

For metal and protein quantification, the pellets were resuspended in demineralized water (200 μL) and lysed for 30 min by ultrasonication. The protein content of cell lysates was determined by the Bradford method. For the ruthenium measurements a contrAA 700 high-resolution continuum-source atomic absorption spectrometer (Analytik Jena AG) was used. All reagents were purchased from Sigma Aldrich. Stock solutions of the respective complexes in graded concentrations (solvent: DMSO) were used as standards and calibration was done in a matrix-matched manner. Meaning all samples and standards were adjusted to the same cellular protein concentration (1.0 mg cell protein per mL) by dilution (final DMSO concentration: 0.5 %). Triton X-100 (1%, 10 μL) as well as nitric acid (13%, 10 μL), were added to each standard sample (120 μL). Samples were injected (50 μL) into coated standard graphite tubes (Analytik Jena AG) and thermally processed as previously described by Schatzschneider *et al.*[7] Drying steps were adjusted ant de atomization temperature set to 2400 °C. Ruthenium was quantified at a wavelength of 349.90 nm. The mean integrated absorbance of double injections was used throughout the measurements. The data of three independent biological replications was used to obtain the uptake values, calculated as nmol metal (ruthenium) per mg cell protein.

AI.6 References

1 A. Bahreman, B. Limburg, M. A. Siegler, E. Bouwman, and S. Bonnet, *Inorg. Chem.* **2013**, 52 (16), 9456-69.

2 A. Bahreman, J.-A. Cuello-Garibo, and S. Bonnet, *Dalton Trans.* **2014**, 43 (11), 4494-4505.

3 J. Snellenburg, J., S. Laptenok, R. Seger, K. Mullen, M., and I. Van Stokkum, H.M., *J. Stat. Softw.* **2012**, 49 (3), 1-22.

4 D. Garcìa-Fresnadillo, Y. Georgiadou, G. Orellana, A. M. Braun, and E. Oliveros, *Helv. Chim. Acta* **1996**, 79 (4), 1222-1238.

5 V. Vichai and K. Kirtikara, *Nat. Protoc.* **2006**, 1 (3), 1112-1116.

6 S. Hopkins, B. Siewert, S. Askes, P. Veldhuizen, R. Zwier, M. Heger, and S. Bonnet, *Photochem. Photobiol. Sci.* **2016**, 15 (5), 644-653.

7 U. Schatzschneider, J. Niesel, I. Ott, R. Gust, H. Alborzinia, and S. Wölfl, *ChemMedChem* **2008**, 3 (7), 1104-1109.

APPENDIX II: SUPPORTING INFORMATION FOR CHAPTER 2

AII.1 ^{1}H NMR spectra

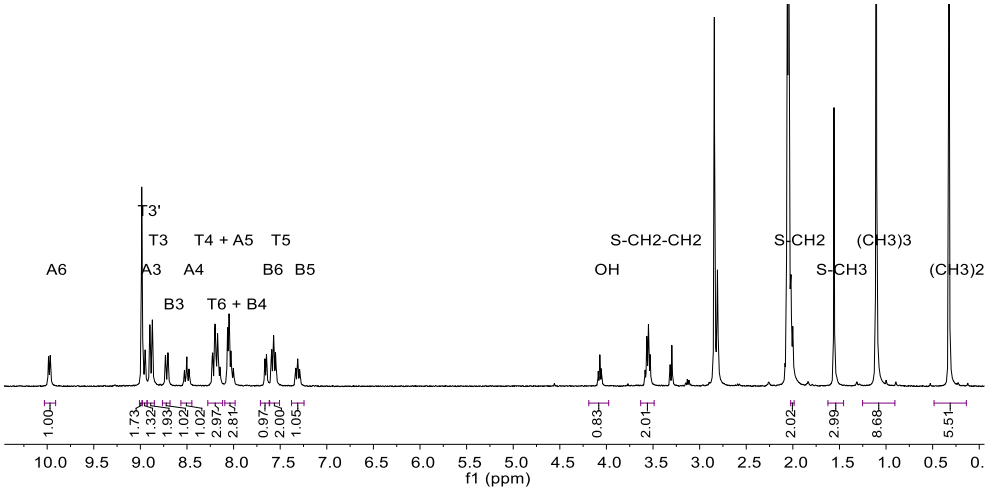

Figure AII.1. ^{1}H NMR spectrum (region 10.5 – 0.0 ppm) of a solution of **[5]**$(PF_6)_2$ in acetone-d_6.

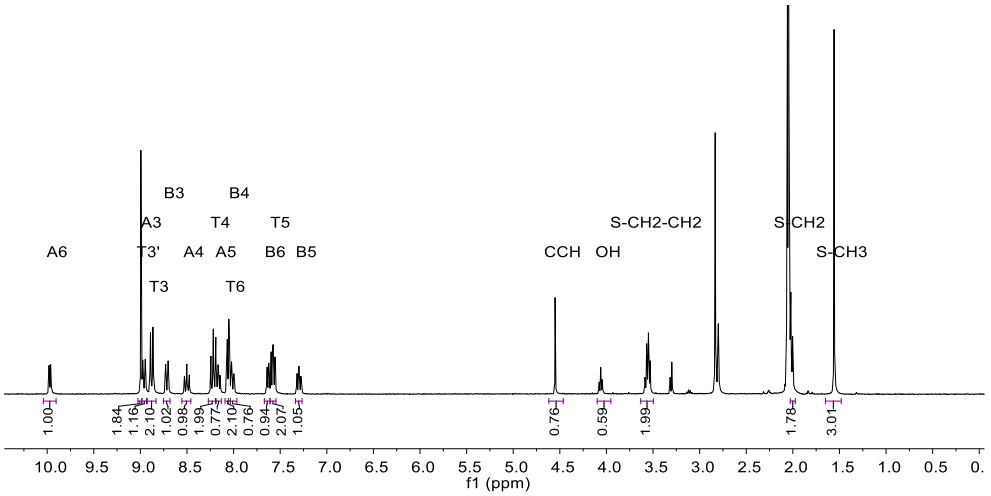

Figure AII.2. ^{1}H NMR spectrum (region 10.5 – 0.0 ppm) of a solution of **[2]**$(PF_6)_2$ in acetone-d_6.

AII.2 Enol ester formation catalyzed by ruthenium

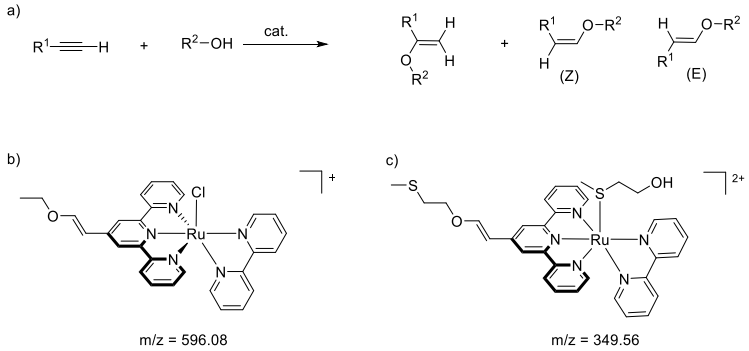

Scheme AII.1. a) General overview of reaction between terminal alkyne and alcohol, catalyzed by ruthenium, and possible products as described by Ruppin *et al*.[1] b) Byproduct observed by mass spectrometry during the coordination of bpy to [Ru(RCC-tpy)$(Cl)_3$] in ethanol/water (3:1) at reflux. TMS is not strong enough as protecting group for the terminal alkyne, allowing ethanol to react with the free alkyne generated in situ. The labile chloride ligand can easily be exchanged, creating a free coordination site on the ruthenium center. c) Byproduct during the exchange reaction of chloride for Hmte in water at 80 °C with an excess of Hmte present that can react with the free alkyne.

AII.3 Dark stability

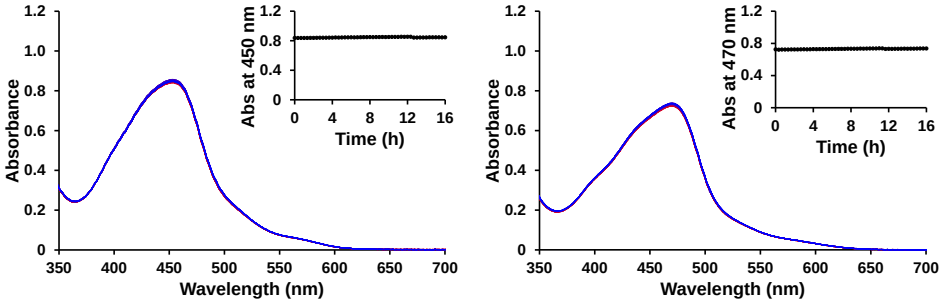

Figure AII.3. Evolution of the UV-vis spectra (region 350 – 700 nm) of a solution of [**1**](PF$_6$)$_2$ (left) or [**2**](PF$_6$)$_2$ (right) in water in the dark. Conditions: [Ru]$_0$ = 0.14 and 0.084 mM for [**1**](PF$_6$)$_2$ and [**2**](PF$_6$)$_2$, respectively, t = 16 h, T = 37 °C, V = 3 mL, under air atmosphere. Inset: Time evolution of absorbance at wavelength 450 nm for [**1**](PF$_6$)$_2$ and 470 nm for [**2**](PF$_6$)$_2$.

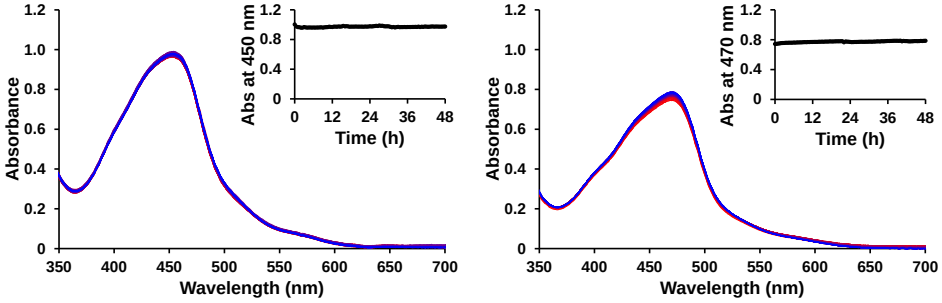

Figure AII.4. Evolution of the UV-vis spectra (region 350 – 700 nm) of a solution of [**1**](PF$_6$)$_2$ (left) and [**2**](PF$_6$)$_2$ (right) in PBS buffer in the dark. Conditions: [Ru]$_0$ = 0.15 and 0.089 mM for [**1**](PF$_6$)$_2$ and [**2**](PF$_6$)$_2$, respectively, t = 48 h, T = 37 °C, V = 3 mL, under air atmosphere. Inset: Time evolution of absorbance at wavelength 450 nm for [**1**](PF$_6$)$_2$ and 470 nm for [**2**](PF$_6$)$_2$.

AII.4 MS after green light activation

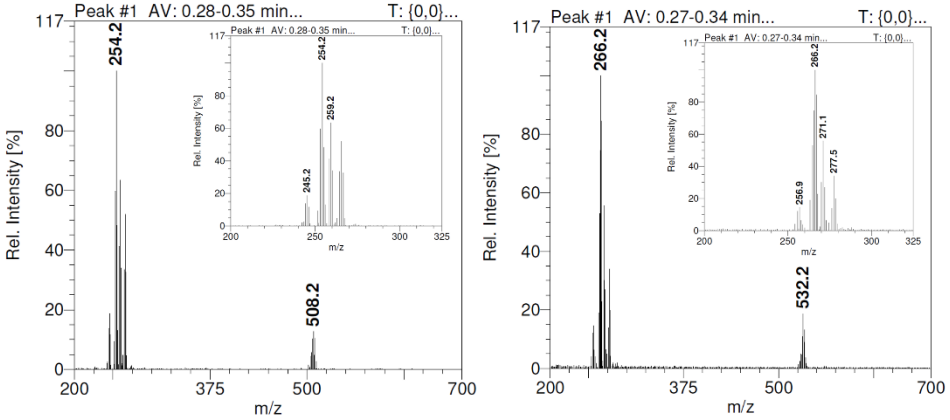

Figure AII.5. Mass spectrum of a solution of [**1**](PF$_6$)$_2$ or [**2**](PF$_6$)$_2$ in water after 70 min of light irradiation at 310 K with a 517 nm LED (5.42 mW, photon flux $\Phi_{517} = 5.4 \cdot 10^{-8}$ mol · s^{-1}) under air atmosphere with peaks corresponding to a) [Ru(tpy)(bpy)(OH$_2$)]$^{2+}$ (calc. m/z = 254.5) and [Ru(tpy)(bpy)(OH)]$^{+}$ (calc. m/z = 508.1); and b) [Ru(HCC-tpy)(bpy)(OH$_2$)]$^{2+}$ (calc. m/z = 266.5) and [Ru(HCC-tpy)(bpy)(OH)]$^{+}$ (calc. m/z = 532.0).

AII.5 Singlet oxygen production and phosphorescence

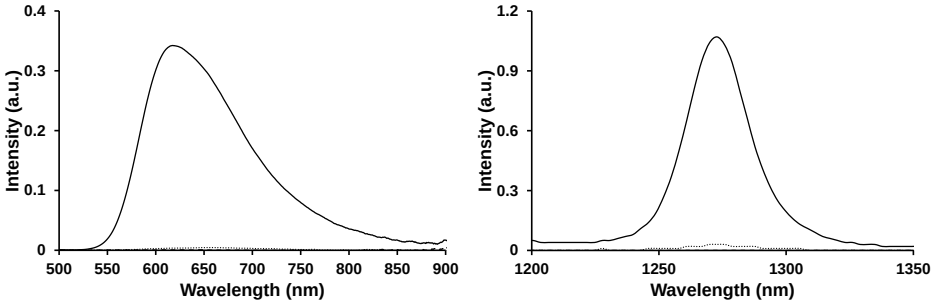

Figure AII.6. Visible emission spectra of [**1**](PF$_6$)$_2$ (···), [**2**](PF$_6$)$_2$ (- -), and [Ru(bpy)$_3$]Cl$_2$ (—) (left) and near-infrared spectra of ^{1}O$_2$ phosphorescence (λ_{em} = 1275 nm) sensitized by [**1**](PF$_6$)$_2$ (···), [**2**](PF$_6$)$_2$ (- -), and [Ru(bpy)$_3$]Cl$_2$ (—) (right) in aerated methanol-d$_4$ at 20 °C under blue-light irradiation (450 nm, 0.4 W · cm^{-2}).

AII.6 CuAAC click reaction with [**2**](PF$_6$)$_2$

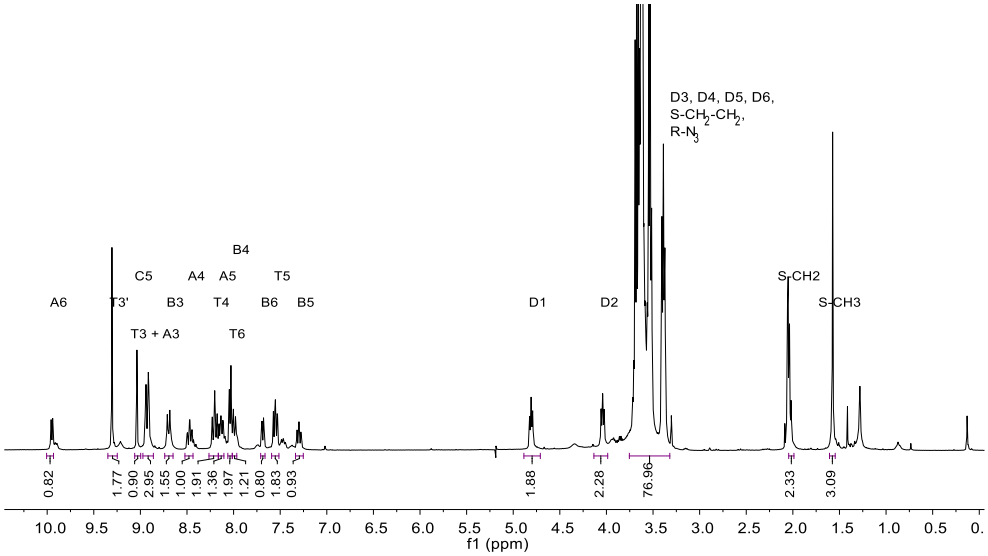

Figure AII.7. ^{1}H NMR spectrum (region 10.5 – 0.0 ppm) of a solution of the click product [**8**](PF$_6$)$_2$ in acetone-d$_6$.

AII.7 Ratio and concentration optimization

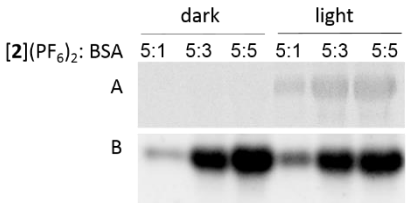

Figure AII.8. SDS PAGE analysis for optimization of ratio between [**2**](PF$_6$)$_2$ (50 μM) and BSA (10, 30 or 50 μM) before and after light activation (520 nm, 1 h, 76 J/cm^2). Click reactions were performed as described under section 2.4.6. Fluorescence labeling (A) and Coomassie blue staining (B).

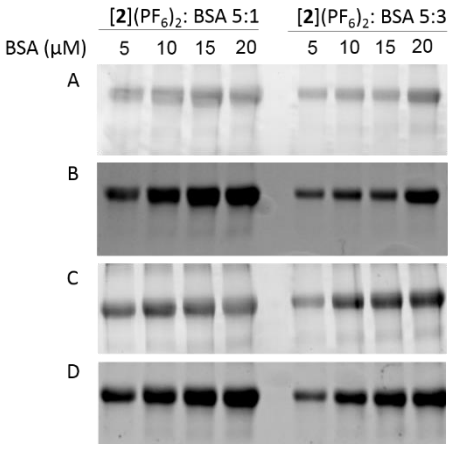

Figure AII.9. SDS PAGE for optimization of concentration of **[2]**$(PF_6)_2$ and BSA at ratio 5:1 or 5:3 after light activation (520 nm, 1 h, 76 J/cm^2). Click reactions were performed as described under 2.4.5. Fluorescence labeling (A) and (C) and Coomassie blue staining (B) and (D) after 6 h and 24 h incubation after light activation, respectively.

AII.8 UV-vis spectra Ru:BSA interaction

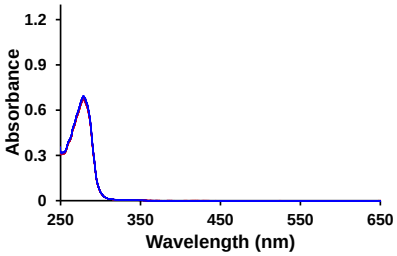

Figure AII.10. Evolution of the UV-vis spectra (region 250 – 650 nm) of a solution of BSA (0.015 mM) in PBS under air atmosphere for 24 h at 37 °C.

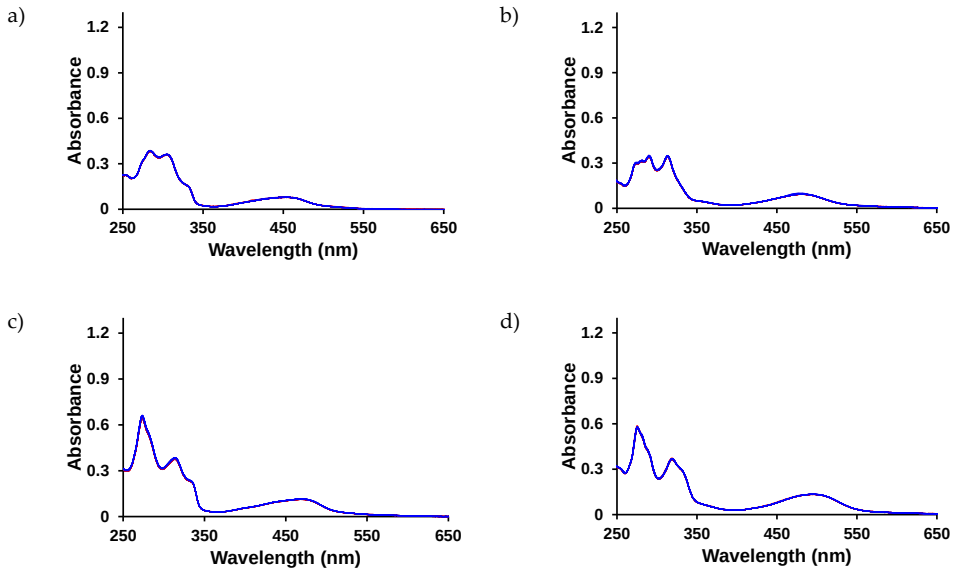

Figure AII.11. Evolution of the UV-vis spectra (region 250 – 650 nm) of a solution of ruthenium complex (0.015 mM) in PBS under air atmosphere for 24 h at 37 °C. a) **[1]**$(PF_6)_2$, b) **[6]**$^{2+}$, c) **[2]**$(PF_6)_2$, d) **[7]**$^{2+}$.

AII.9 ESI MS spectra Ru:BSA interaction

Table AII.1. ICP-AES quantification of ruthenium bound to BSA.

Compound	Ru (g)	Ru (mol)	BSA (mol)	BSA/Ru ratio (mol/mol)
[7]$^{2+}$	$1.13 \cdot 10^{-6}$	$1.12 \cdot 10^{-8}$	$9.0 \cdot 10^{-8}$	1:0.12
[2]$^{2+}$	$3.77 \cdot 10^{-6}$	$3.73 \cdot 10^{-8}$		1: 0.41
[6]$^{2+}$	$3.01 \cdot 10^{-7}$	$2.97 \cdot 10^{-9}$		1: 0.03
[1]$^{2+}$	$3.31 \cdot 10^{-7}$	$3.27 \cdot 10^{-9}$		1: 0.04

APPENDIX III: SUPPORTING INFORMATION FOR CHAPTER 3

III.1 Synthetic route

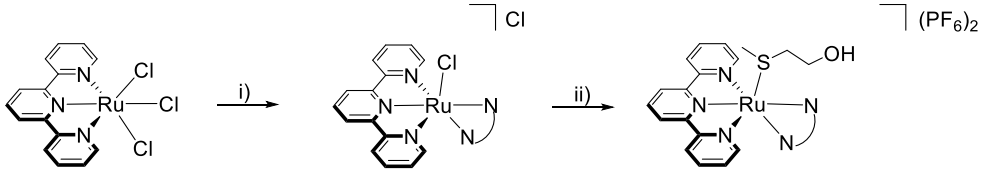

Scheme AIII.1. Route for the synthesis of [**2**](PF$_6$)$_2$ and [**3**](PF$_6$)$_2$. Conditions: (i) LiCl, Et$_3$N, ethanol/water (3:1), N$_2$, reflux, i-biq (overnight, 94%) or i-Hdiqa (4 h, 83%); (ii) Hmte, AgPF$_6$, water, N$_2$, reflux, 4 h for [**2**](PF$_6$)$_2$ (48%) and 3 h for [**3**](PF$_6$)$_2$ (60%).

III.2 Dark stability in water and OptiMEM

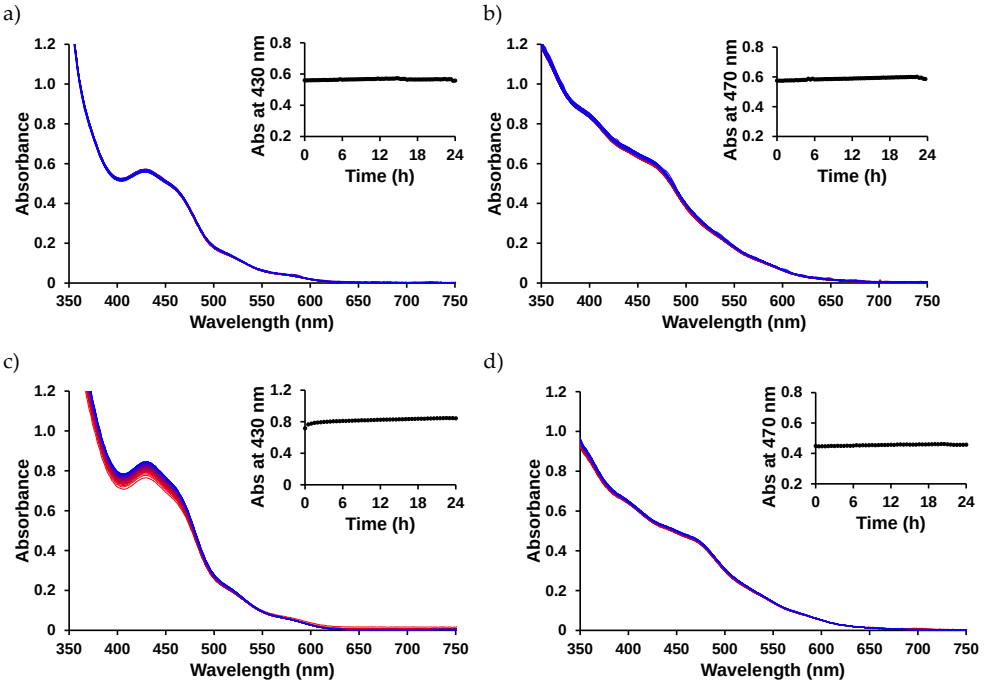

Figure AIII.1. Evolution of the UV-vis spectra (region 350 – 750 nm) of a solution of a) [**2**](PF$_6$)$_2$ and b) [**3**](PF$_6$)$_2$ in water, and c) [**2**](PF$_6$)$_2$ and d) [**3**](PF$_6$)$_2$ in OptiMEM complete. Conditions: [Ru] = 0.097, 0.104, 133, and 0.081 mM, respectively, T = 37 °C, t = 24 h, V = 3 mL, under air atmosphere and in the dark. Inset: Time evolution of absorbance at wavelength 430nm for [**2**](PF$_6$)$_2$ and 470 nm for [**3**](PF$_6$)$_2$.

III.3 Molar extinction coefficient in water

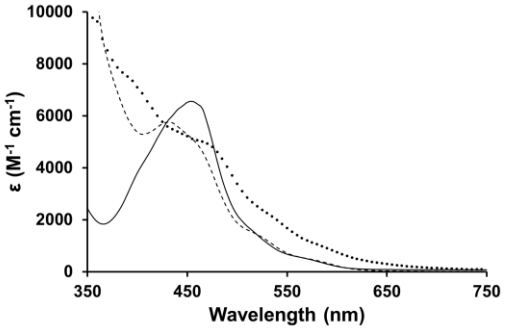

Figure AIII.2. Molar absorbance of solutions of [**1**]$(PF_6)_2$ (---), [**2**]$(PF_6)_2$ (- -), and [**3**]$(PF_6)_2$ (· ·) in water.

III.4 Singlet oxygen production and phosphorescence

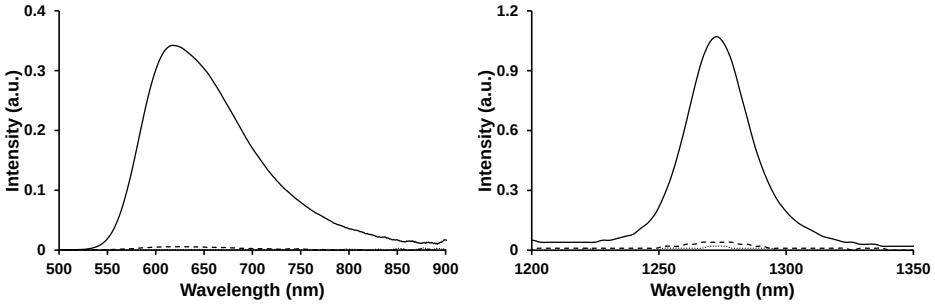

Figure AIII.3. Visible emission spectra (left) of and near-infrared spectra of $^1O_2$ phosphorescence (λ_{em} = 1275 nm) (right) sensitized by [**2**]$(PF_6)_2$ (···), [**3**]$(PF_6)_2$ (- -), and $[Ru(bpy)_3]Cl_2$ (—) in aerated methanol-d_4 at 293 K under blue-light irradiation (450 nm, 0.4 W · cm^{-2}).

III.5 MS of the ruthenium species after green light irradiation

a) b)

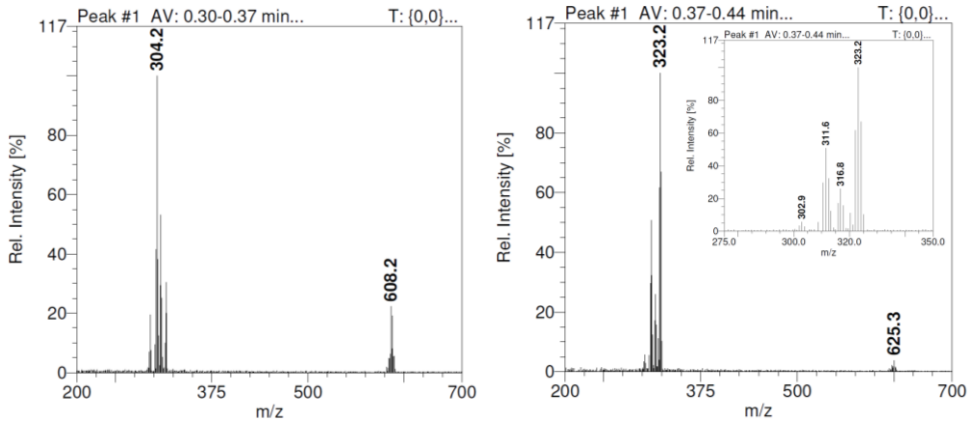

Figure AIII.4. Mass spectrum of a solution of **[2]**$(PF_6)_2$ and **[3]**$(PF_6)_2$ in water after 50 min of light irradiation at 310 K with a 517 nm LED with a photon flux of $\Phi_{517} = 5.2 \cdot 10^{-8}$ mol $\cdot$ s^{-1} under air atmosphere. Peaks corresponding to a) $[Ru(tpy)(i\text{-}biq)(OH_2)]^{2+}$ (calc. m/z = 304.5) and $[Ru(tpy)(i\text{-}biq)(OH)]^{+}$ (calc. m/z = 608.1); and b) $[Ru(tpy)(i\text{-}Hdiqa)(OH_2)]^{2+}$ (calc. m/z = 312.1) and $[Ru(tpy)(i\text{-}Hdiqa)(OH)]^{+}$ (calc. m/z = 623.1). $[Ru(tpy)(i\text{-}Hdiqa)(MeCN)]^{2+}$ (calc. m/z = 323.6).

III.6 Photosubstitution quantum yield simulated by Glotaran

Table AIII.1. Conditions of the photoreactions used for Glotaran calculations.

	[2]$(PF_6)_2$	**[3]$(PF_6)_2$**
irradiation wavelength (λ in nm)	517	517
volume (V in L)	0.003	0.003
path length (l in m)	0.01	0.01
concentration (c in M)	$7.41 \cdot 10^{-5}$	$6.11 \cdot 10^{-5}$
photon flux (Φ in mol $\cdot$ s^{-1})	$5.2 \cdot 10^{-8}$	$5.2 \cdot 10^{-8}$
epsilon Ru-L (ε in M$^{-1} \cdot$ cm^{-1}) at 517 nm	1435	2651
epsilon Ru-OH_2 (ε in M$^{-1} \cdot$ cm^{-1}) at 517 nm	3305	5025

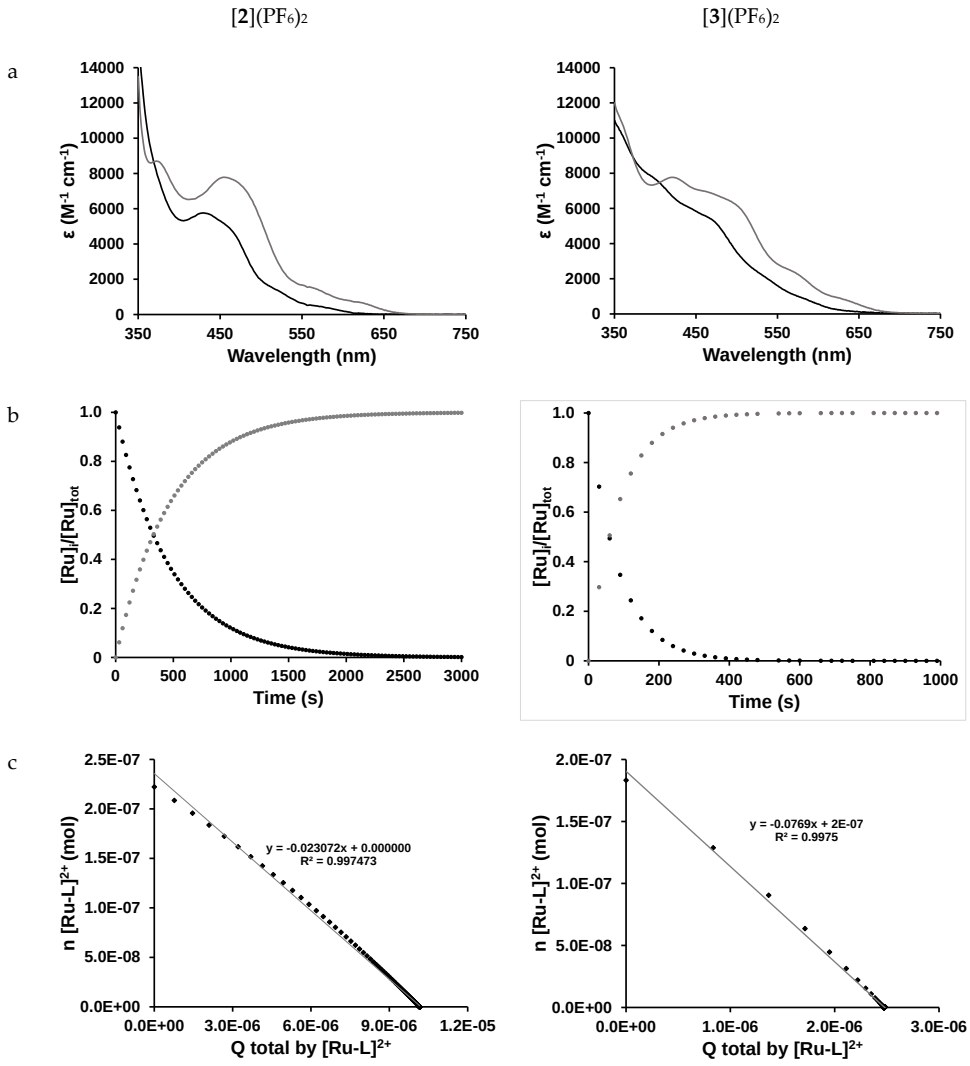

Figure AIII.5. Kinetic data for the photosubstitution of Hmte according to the time evolution of the absorbance spectra of solutions of [**2**](PF$_6$)$_2$ and [**3**](PF$_6$)$_2$ in H$_2$O irradiated with green light under air atmosphere. a) Globally fitted absorption spectra of the starting material [**2**](PF$_6$)$_2$ and [**3**](PF$_6$)$_2$ (black) and their aqua products [Ru(tpy)(NN)(H$_2$O)]$^{2+}$ ([**5**]$^{2+}$ and [**6**]$^{2+}$, grey). b) Modelled evolution of the relative concentration of [**2**]$^{2+}$ and [**3**]$^{2+}$ *vs.* irradiation time according to global fitting using Glotaran. c) Plot of the amount of [**2**]$^{2+}$ and [**3**]$^{2+}$ (mol) *vs.* total amount of photons absorbed by [**2**]$^{2+}$ and [**3**]$^{2+}$ since t = 0 (mol). The slope of the obtained line is the opposite of the quantum yield of the formation for the aqua complex. Conditions: 0.074 and 0.061 mM solution of [**2**](PF$_6$)$_2$ and [**3**](PF$_6$)$_2$ in MilliQ H$_2$O irradiated at 298 K under air atmosphere using a 517 nm LED.

III.7 Determination of light dose

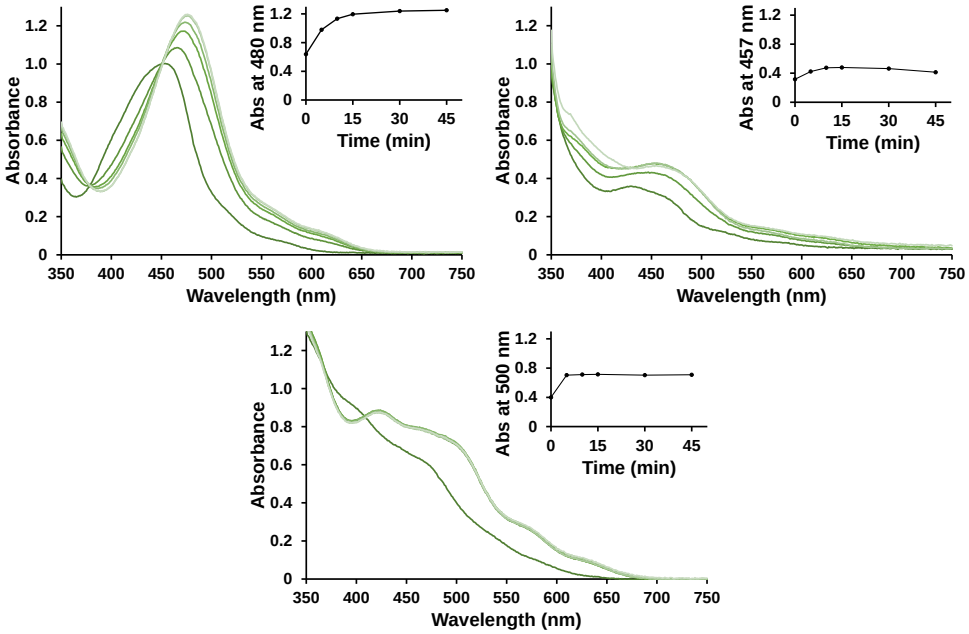

Figure AIII.6. Evolution of the UV-vis spectra (region 350 – 750 nm) of solutions of [**1**](PF$_6$)$_2$, [**2**](PF$_6$)$_2$, and [**3**](PF$_6$)$_2$ in demineralized water upon green light irradiation in a 96 well plate, *i.e.* under the conditions of the cytotoxicity experiment. Conditions: [Ru] = 250 μM, T = 37 °C, t = 0, 5, 10, 15, 30, and 45 min, light source: λ = 520 ± 20 nm, 20.9 ± 1.6 mW · cm^{-2}, V = 200 μL, under air atmosphere. Inset: Time dependent absorbance at wavelength 480 nm for [**1**](PF$_6$)$_2$, 457 nm for [**2**](PF$_6$)$_2$, and 500 nm for [**3**](PF$_6$)$_2$.

III.8 Dose response curves

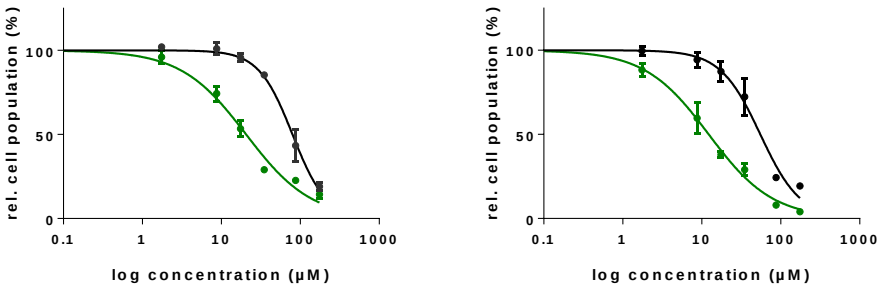

Figure AIII.7. Dose response curves for A549 (left) and A431 (right) cells under normoxia treated with [**2**](PF$_6$)$_2$ and irradiated with green light (520 nm, 38 J · cm^{-2}) 24 h after treatment (green line) or left in the dark (black line).

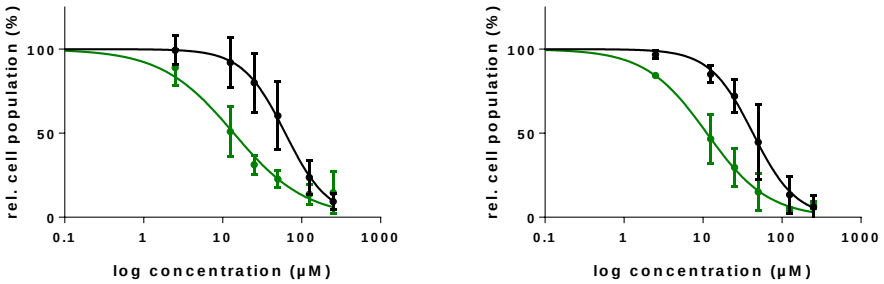

Figure AIII.8. Dose response curves for A549 (left) and A431 (right) cells under normoxia treated with [**3**](PF$_6$)$_2$ and irradiated with green light (520 nm, 38 J · cm^{-2}) 24 h after treatment (green line) or left in the dark (black line).

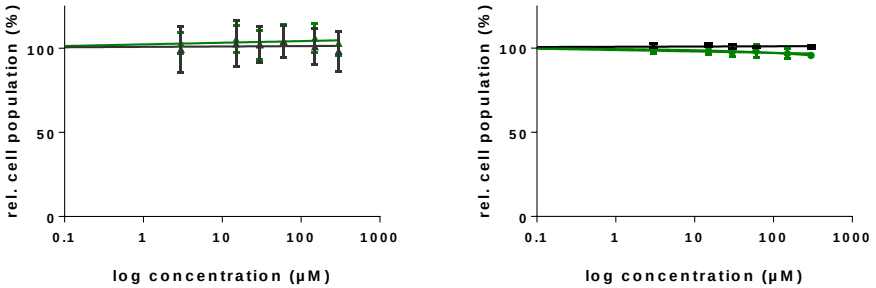

Figure AIII.9. Dose response curves for A549 (left) and A431 (right) cells under normoxia treated with Hmte and irradiated with green light (520 nm, 38 J · cm^{-2}) 24 h after treatment (green line) or left in the dark (black line).

III.9 DFT models

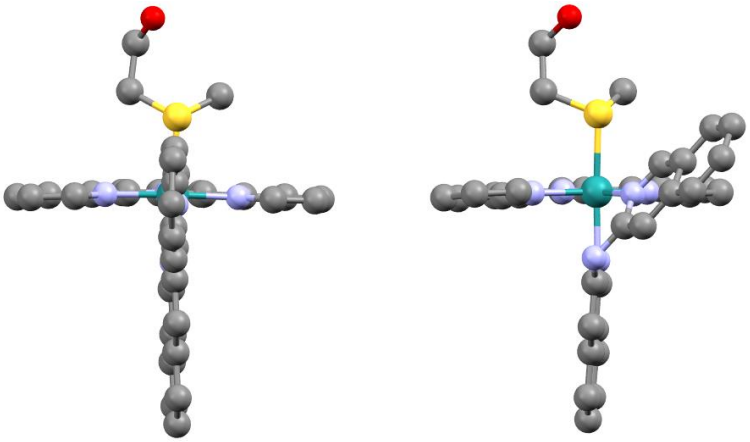

Figure AIII.10. Structure of [**2**]$^{2+}$ (left) and [**3**]$^{2+}$ (right) optimized by DFT in water (PBE0/TZP/COSMO).

Table AIII.2. Nuclear coordinates (Å) of $[\mathbf{2}]^{2+}$ minimized at the DFT/PBE0/TZP/COSMO level in water.

Ru	0.2083679912835394	0.1173257488624371	-0.4497260606369664
C	2.617688291197344	1.551691430961221	0.8778959156333664
H	1.857834723905196	2.194107365239715	1.303929122195062
C	3.960724497568178	1.757383403522149	1.140285727173813
H	4.259364033605204	2.574252274544991	1.783782159741243
C	4.891346110905469	0.9093727917714107	0.5645562903325541
H	5.950558632083908	1.044179909507778	0.7443494360975174
C	4.449423115777398	-0.1204577020940638	-0.2487779181973365
H	5.155694252807213	-0.7977375012028864	-0.7088039053973125
C	3.090989925868592	-0.2730406395506106	-0.4753439169672215
C	2.533237691960434	-1.335857551720791	-1.328301706298766
C	3.24285674836314	-2.335225550213443	-1.978912100918067
H	4.32070659561827	-2.385278263505907	-1.911214340227477
C	2.541408426845852	-3.2790411417088	-2.71469642305054
H	3.077944774229405	-4.064769733795076	-3.231211161867237
C	1.156996670256847	-3.232433503697451	-2.780687894325799
H	0.6099674258378032	-3.979493832041498	-3.33905212121223
C	0.4914302203796511	-2.215204872614736	-2.110663654230446
C	-0.9663137900903168	-2.026747110554691	-2.028111322046999
C	-1.874312333061412	-2.881566233875994	-2.63310977491304
H	-1.523919404415143	-3.729021445980387	-3.205898770903363
C	-3.23104238745723	-2.642827798302436	-2.493237908275751
H	-3.951118650153515	-3.303471327805739	-2.959801392166215
C	-3.646801608685728	-1.552403023972211	-1.748574323300601
H	-4.695930715786754	-1.327391176975751	-1.608973696487936
C	-2.691418078707873	-0.735645884162886	-1.170154147794213
H	-2.976950582867617	0.1268942144785017	-0.5821875845477985
N	2.181101327220925	0.5696892440728344	0.08564824812676824
N	1.193127783541921	-1.292947215174845	-1.428454131776693
N	-1.380273947620814	-0.9533329238833577	-1.300656196754388
C	-1.393471196027837	2.620438170814063	0.4042623143945007
H	-1.123517509182634	2.982728791416989	-0.5810566183846197
C	-2.224418866223735	3.405665344486646	1.222109528721864
C	-2.731133568375314	4.652450412072225	0.7970144697214701
H	-2.468443933913542	5.02654395471265	-0.1860829517911313
C	-3.549338171103099	5.368288412613389	1.628822890872407
H	-3.945387392170889	6.32499123524617	1.309115936429985
C	-3.88659000780193	4.869922864403923	2.906130137038371
H	-4.536344582108921	5.453683178073768	3.548019418805768
C	-3.405350469976215	3.663905255783805	3.340981060735985
H	-3.66480327149348	3.281463589915676	4.321561084089738
C	-2.56174053922833	2.902782978070626	2.502551807086794
C	-2.036867370346503	1.651496909829876	2.867256944336066
H	-2.286884652361376	1.243146706633071	3.83718914403587

C	-1.234445289862512	0.9509121106635542	2.004871535615553
C	-0.6746534617535808	-0.3656145324083772	2.327139504982696
C	-0.8120766943186178	-0.9670797830453756	3.551022905313966
H	-1.345504549671184	-0.4692047206310123	4.349612189657306
C	-0.2576293826036777	-2.23558456112777	3.793765811601495
C	-0.3627007341662732	-2.902001914470313	5.034634070331201
H	-0.8953416259472317	-2.42567385196123	5.849745089448689
C	0.2068437316836899	-4.137077308358533	5.193449610592506
H	0.1269353185372501	-4.648526270948042	6.14575587128791
C	0.9009830081163462	-4.759006110143837	4.133027000650242
H	1.342220211706593	-5.73671420002553	4.286629201206821
C	1.018922983066359	-4.136117889852509	2.920213002683382
H	1.551252541269151	-4.605643235267709	2.100633046145049
C	0.440979876583827	-2.86258273534604	2.733079986925966
C	0.5381980767687432	-2.170445857365483	1.514638400497948
H	1.072812194832305	-2.626424479700958	0.6905127176816017
N	-0.9158350918367943	1.443457645808958	0.7573950146199396
N	0.01568183074122983	-0.9802156170868606	1.309043635434526
C	2.039591911060169	1.894933036207212	-2.793011015717027
H	2.479452552716376	0.9574003560668584	-3.129175837202628
H	2.585227519727869	2.284298858196861	-1.937192715796087
H	2.058902075030991	2.634795642469756	-3.589979927944774
S	0.3282090149283553	1.670940353476732	-2.269301183090305
C	-0.398815967668077	0.9542844710175553	-3.777184870498797
H	-0.1197380759669304	-0.09748519177659898	-3.853889739659892
H	-1.4766145139828	1.014202997494053	-3.616679799483083
C	0.004354563648658137	1.653403455773825	-5.063472499084149
H	1.051528319682407	1.454367110703531	-5.289316150214599
H	-0.5900092427384502	1.215525147282966	-5.871739545699212
O	-0.132554221558341	3.063845517400228	-5.03379825696929
H	-1.072162150087336	3.275246969664708	-4.971018119851347

Table AIII.3. Nuclear coordinates (Å) of [**3**]$^{2+}$ minimized at the DFT/PBE0/TZP/COSMO level in water.

Ru	0.161709	0.107889	-0.624947
C	2.534685	1.634117	0.6795
H	1.759708	2.227168	1.147331
C	3.87283	1.908686	0.900925
H	4.14734	2.731564	1.547451
C	4.828243	1.119831	0.284229
H	5.884184	1.30953	0.430199
C	4.414284	0.07201299999999999	-0.520744
H	5.139515	-0.567732	-1.004342
C	3.059003	-0.151129	-0.704146
C	2.531576	-1.261463	-1.513959
C	3.276551	-2.245425	-2.148115

H	4.357141	-2.23066	-2.117325000000001
C	2.607317	-3.260847	-2.815113
H	3.171099	-4.038527	-3.314433
C	1.221694	-3.291515	-2.836848
H	0.70038	-4.089249	-3.3476
C	0.520649	-2.280657	-2.193243
C	-0.942152	-2.135796	-2.13235
C	-1.809778	-3.03867	-2.727602
H	-1.421817	-3.91215	-3.233121
C	-3.17354	-2.8087	-2.673833
H	-3.862786	-3.506292	-3.133235
C	-3.634027	-1.670487	-2.035314
H	-4.689488	-1.438774	-1.978518
C	-2.717003	-0.814173	-1.451956
H	-3.042935	0.08209	-0.943654
N	2.122056	0.642547	-0.113939
N	1.187603	-1.296183	-1.567129
N	-1.399724	-1.033302	-1.478919
C	-0.784934	2.883257	0.251161
H	0.018774	3.174929	-0.413982
C	-1.593178	3.879968	0.809882
C	-1.387706	5.2529	0.538616
H	-0.571385	5.548936	-0.110979
C	-2.220565	6.183609000000001	1.092671
H	-2.073204	7.237455	0.888224
C	-3.282525	5.779798	1.935187
H	-3.93175	6.534141	2.365079
C	-3.501556	4.458668	2.214762
H	-4.316191	4.154731	2.86234
C	-2.657993	3.472143	1.653635
C	-2.790482	2.099351	1.905009
H	-3.55748	1.740296	2.581217
C	-1.937868	1.201067	1.310411
C	-1.095307	-1.044427	1.895014
C	-1.271482	-1.887152	2.965573
H	-2.181608	-1.823141	3.550141
C	-0.273561	-2.808106	3.314467
C	-0.3796	-3.706505	4.401566
H	-1.28331	-3.711596	5.000156
C	0.655828	-4.554234	4.687181
H	0.572726	-5.241765	5.521352
C	1.839476	-4.551702	3.912671
H	2.642006	-5.235738	4.162189
C	1.971663	-3.692583	2.858424
H	2.87436	-3.680517	2.25769
C	0.916255	-2.804887	2.54265

C	0.9946120000000001	-1.910447	1.469447
H	1.891249	-1.903154	0.86431
N	-0.954047	1.583713	0.446298
N	0.029752	-1.072408	1.125377
C	1.886228	1.935304	-3.00795
H	2.417364	1.030255	-3.298116
H	2.375263	2.401652	-2.155578
H	1.862595	2.645112	-3.831636
S	0.187945	1.578699	-2.516694
C	-0.418341	0.724009	-4.006151
H	-0.027849	-0.294179	-4.028884
H	-1.500273	0.67875	-3.874731
C	-0.053696	1.409174	-5.310998000000001
H	1.014585	1.315088	-5.502802
H	-0.5744469999999999	0.876715	-6.113368
O	-0.342038	2.7963	-5.345442
H	-1.300419	2.906381	-5.312955
N	-2.113618	-0.161765	1.543382
H	-2.942264	-0.329492	2.096443

AIII.10 References

1 C. Ruppin and P. H. Dixneuf, *Tetrahedron Lett.* **1986**, 27 (52), 6323-6324.

2 R. Wirth, J. D. White, A. D. Moghaddam, A. L. Ginzburg, L. N. Zakharov, M. M. Haley and V. J. DeRose, *J. Am. Chem. Soc.* **2015**, 137 (48), 15169-15175.

APPENDIX IV:SUPPORTING INFORMATION FOR CHAPTER 4

AIV.1 Synthesis

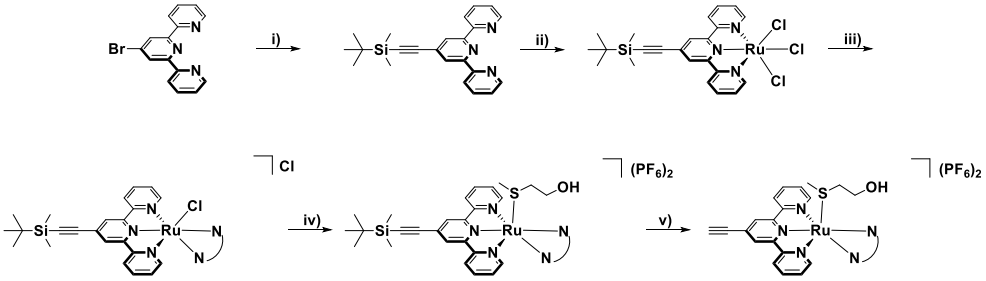

Scheme AIV.1. Reaction scheme of the stepwise synthesis of [**2**]$(PF_6)_2$ and [**4**]$(PF_6)_2$. Conditions: i) CuI, $Pd(PPh_3)_2Cl_2$, TBDMS-ethyne, Et_3N, 80 °C, N_2, 7 h, 95%; ii) $RuCl_3$, ethanol, 80 °C, 16 h, 75%; iii) LiCl, Et_3N, ethanol/water (3:1), 60 °C, i-biq (overnight, 73%) or i-Hdiqa (5 h, 71%); (iv) Hmte, water, 60 °C, N_2, 16 h, aq. KPF_6; 93 and 95%, respectively; v) KF, methanol, 30 °C, 16 h, aq. KPF_6; 82 and 83%, respectively.

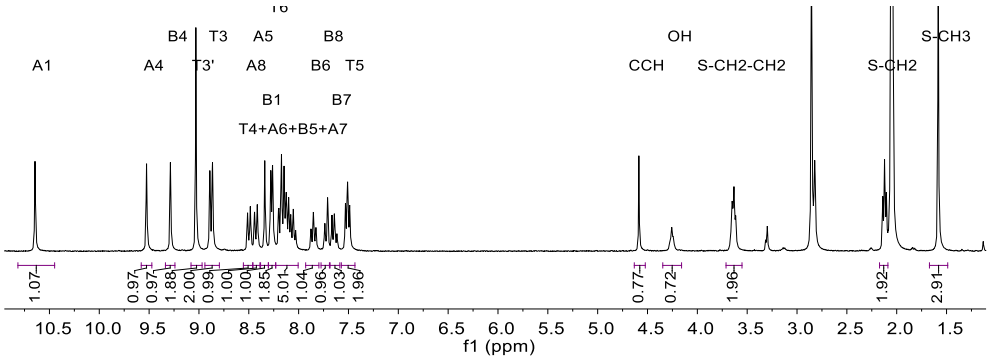

Figure AIV.1. ^1H NMR spectrum (region 11.0 – 1.0 ppm) of a solution of [**2**]$(PF_6)_2$ in acetone-d_6 at 25 °C. Atom numbering as donated in the experimental section 4.4.2.

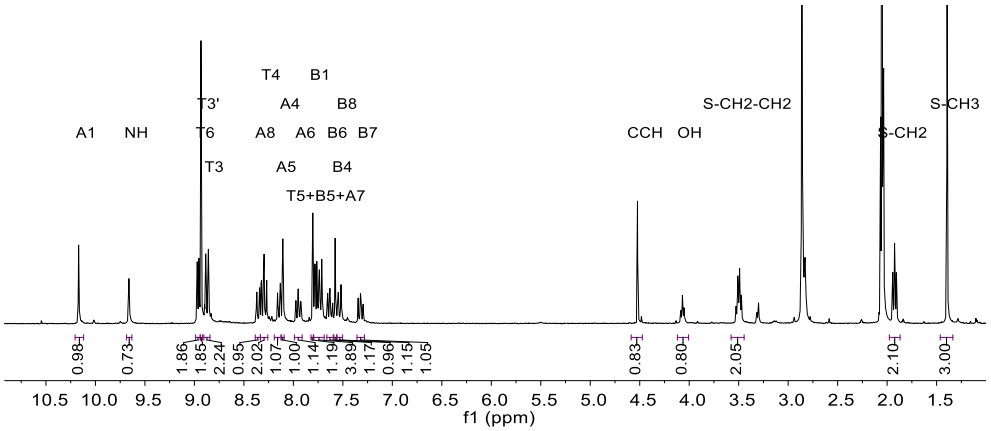

Figure AIV.2. ^{1}H NMR spectrum (region 11.0 – 1.0 ppm) of a solution of [**4**](PF$_6$)$_2$ in acetone-d$_6$ at 25 °C. Atom numbering according to the experimental section 4.4.2.

AIV.2 Molar extinction coefficient in water

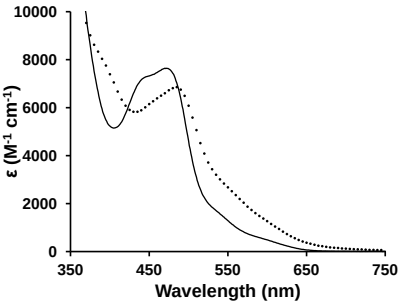

Figure AIV.3. Molar extinction coefficient of aqueous solutions of [**2**]Cl$_2$ (—) and [**4**](PF$_6$)$_2$ (···) in water.

AIV.3 Singlet oxygen production and phosphorescence

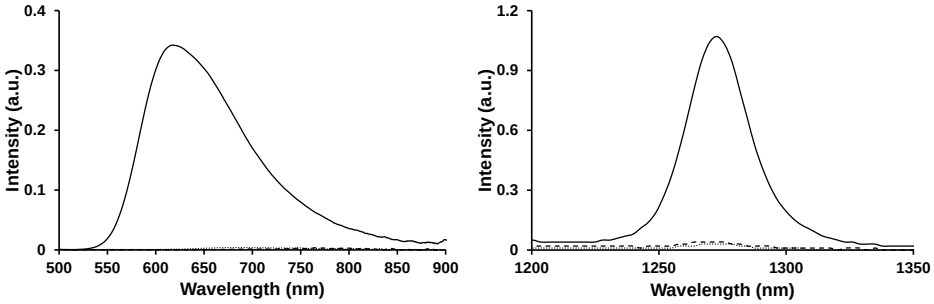

Figure AIV.4. Visible emission spectra of [**2**]Cl$_2$ (···), [**4**](PF$_6$)$_2$ (- -), and [Ru(bpy)$_3$]Cl$_2$ (—) (left) and near-infrared spectra of ^{1}O$_2$ phosphorescence (λ_{em} = 1275 nm) sensitized by [**2**]Cl$_2$ (···), [**4**](PF$_6$)$_2$ (- -), and [Ru(bpy)$_3$]Cl$_2$ (—) (right) in aerated methanol-d$_4$ at 293 K under blue-light irradiation (450 nm, 0.4 W · cm^{-2}).

AIV.4 Green light activation

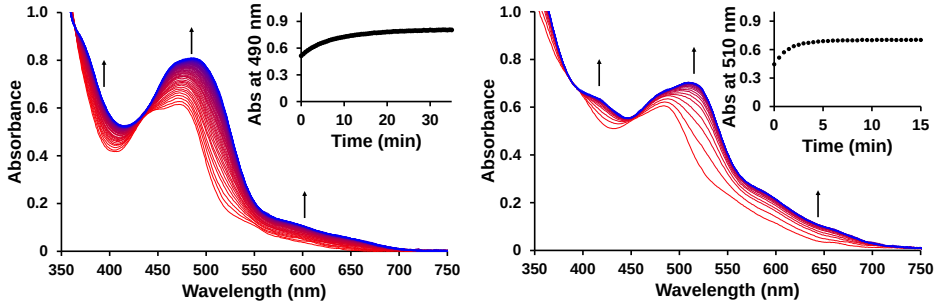

Figure AIV.5. Evolution of the UV-vis absorption spectra of a solution of [**2**]Cl_2 and [**4**]$(PF_6)_2$ in water upon green light irradiation. Conditions: [Ru] = 0.077 and 0.127 mM for [**2**]Cl_2 and [**4**]$(PF_6)_2$, respectively, T = 37 °C, light source: λ = 517 nm, $\Delta\lambda_{1/2}$ = 23 nm, 5.2 mW, photon flux $\Phi_{517} = 5.3 \cdot 10^{-8}$ and $5.2 \cdot 10^{-8}$ mol · s^{-1}, V = 3 mL, under air atmosphere. Inset: Time evolution of absorbance at wavelength 490 nm for [**2**]Cl_2 and 510 nm for [**4**]$(PF_6)_2$.

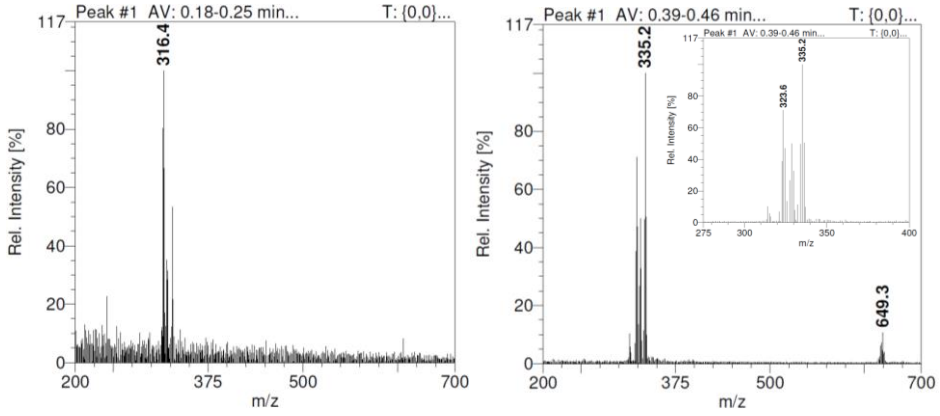

Figure AIV.6. Mass spectrum of a solution of [**2**]Cl_2 and [**4**]$(PF_6)_2$ in water after 80 and 50 min, respectively, of light irradiation at 310 K with a 517 nm LED with a photon flux $\Phi_{517} = 5.3 \cdot 10^{-8}$ and $5.2 \cdot 10^{-8}$ mol · s^{-1}, respectively, under air atmosphere with peaks corresponding to a) $[Ru(HCC\text{-}tpy)(i\text{-}biq)(OH_2)]^{2+}$ (calc. m/z = 316.5); and b) $[Ru(HCC\text{-}tpy)(i\text{-}Hdiqa)(OH_2)]^{2+}$ (calc. m/z = 324.1) and $[Ru(HCC\text{-}tpy)(i\text{-}Hdiqa)(OH)]^{+}$ (calc. m/z = 647.1). $[Ru(HCC\text{-}tpy)(i\text{-}Hdiqa)(MeCN)]^{2+}$ (calc. m/z = 335.6).

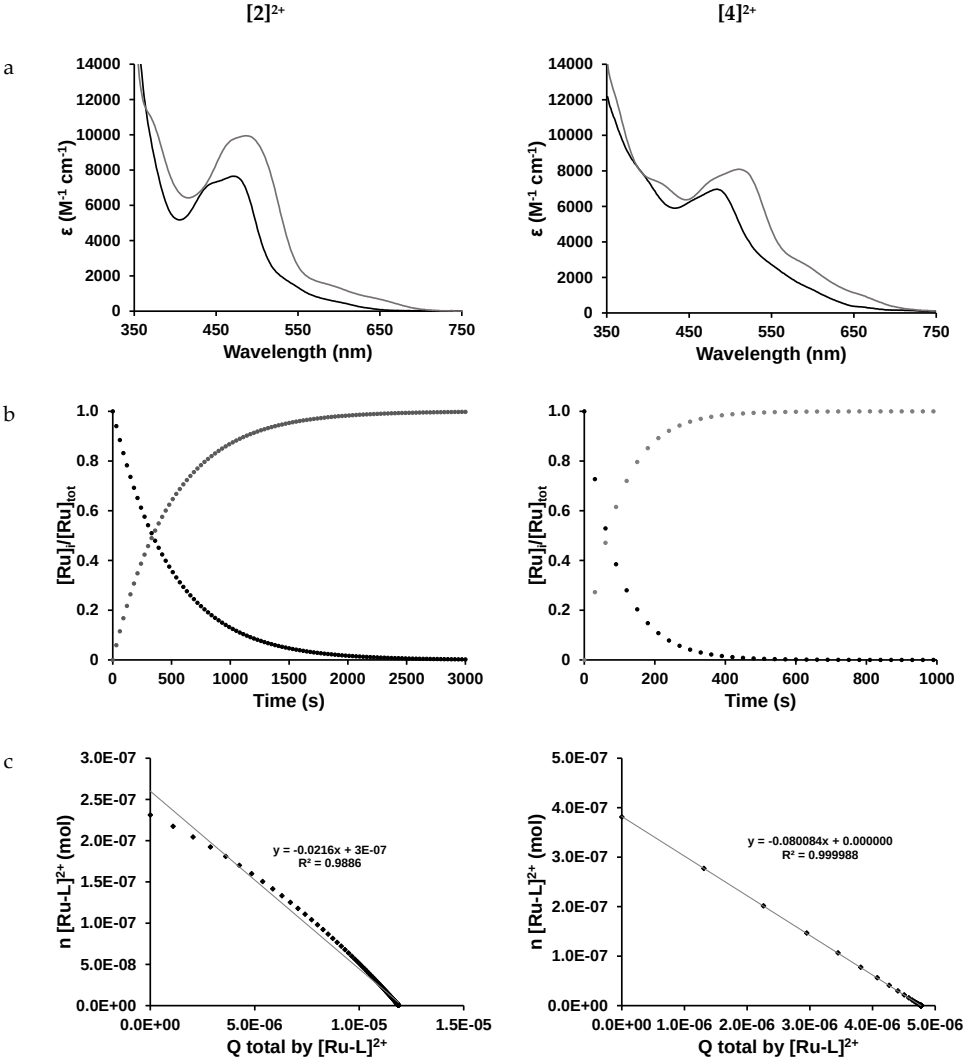

Figure AIV.7. Kinetic data for the photosubstitution of Hmte according to the time evolution of the absorbance spectra of solutions of [**2**]Cl_2 and [**4**]$(PF_6)_2$ in H_2O under air atmosphere. a) Globally fitted absorption spectra of the starting material [**2**]Cl_2 and [**4**]$(PF_6)_2$ (black) and their aqua products [Ru(HCC-tpy)(i-biq)(H_2O)]$^{2+}$ and [Ru(HCC-tpy)(i-Hdiqa)(H_2O)]$^{2+}$ (grey). b) Modelled evolution of the relative concentration of [**2**]$^{2+}$ and [**4**]$^{2+}$ vs. irradiation time according to global fitting using Glotaran. c) Plot of the amount of [**2**]$^{2+}$ and [**4**]$^{2+}$ (mol) vs. total amount of photons absorbed by [**1**]$^{2+}$ and [**3**]$^{2+}$ since t = 0 (mol). The slope of the obtained line is the opposite of the quantum yield of the formation of the aqua complex. Conditions: 0.077 and 0.127 mM solution of [**2**]Cl_2 and [**4**]$(PF_6)_2$ in MilliQ H_2O irradiated at 298 K under air atmosphere using a 517 nm LED.

Table AIV.1. Conditions of the photoreactions used for Glotaran calculations.

	[2]Cl_2	**[4]$(PF_6)_2$**
irradiation wavelength (λ in nm)	517	517
volume (V in L)	0.003	0.003
path length (l in m)	0.01	0.01
concentration (c in M)	$7.71 \cdot 10^{-5}$	$1.27 \cdot 10^{-4}$
photon flux (Φ in mol $\cdot$ s^{-1})	$5.3 \cdot 10^{-8}$	$5.2 \cdot 10^{-8}$
epsilon Ru-L (ε in $M^{-1} \cdot cm^{-1}$) at 517 nm	2531	4458
epsilon Ru-OH_2 (ε in $M^{-1} \cdot cm^{-1}$) at 517 nm	7536	8014

AIV.5 Dark stability

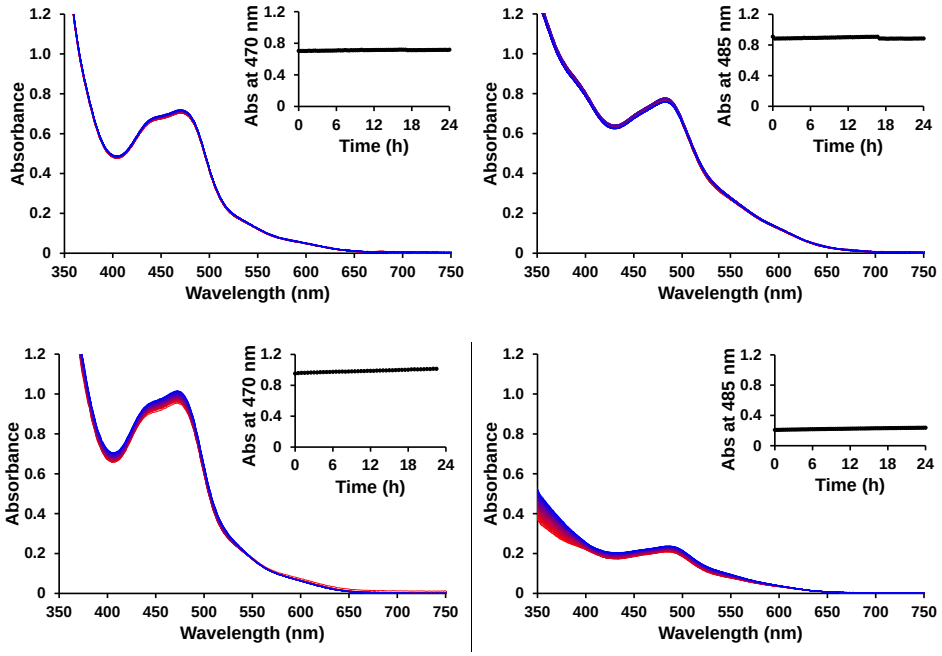

Figure AIV.8. Evolution of the UV-vis spectra (region 350 – 750 nm) of a solution of a) [**2**]Cl_2 and b) [**4**]$(PF_6)_2$ in water, and c) [**2**]Cl_2 and d) [**4**]$(PF_6)_2$ in OptiMEM complete. Conditions: [Ru] = 0.094, 0.111, 0.130, and 0.035 mM, respectively, T = 37 °C, t = 24 h, V = 3 mL, under air atmosphere and in the dark. Inset: Time evolution of absorbance at wavelength 470 nm for [**2**]Cl_2 and 485 nm for [**4**]$(PF_6)_2$.

AIV.6 Determination of light dose

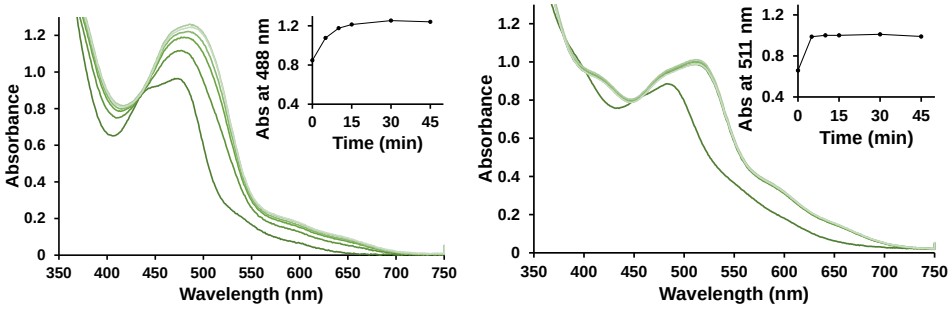

Figure AIV.9. Evolution of the UV-vis spectra (region 350 – 750 nm) of a solution of [**2**]Cl_2 and [**4**]$(PF_6)_2$ in demineralized water upon green light irradiation in a 96 well plate *i.e.* under the conditions of the cytotoxicity experiment. Conditions: [Ru] = 250 μM, T = 37 °C, t = 0, 5, 10, 15, 30, and 45 min, light source: $\lambda = 520 \pm 20$ nm, 20.9 ± 1.6 mW · cm^{-2}, V = 200 μL, under air atmosphere. Inset: Time dependent absorbance at wavelength 488 nm for [**2**]Cl_2 and 511 nm for [**4**]$(PF_6)_2$.

AIV.7 Dose response curves for A549 cells

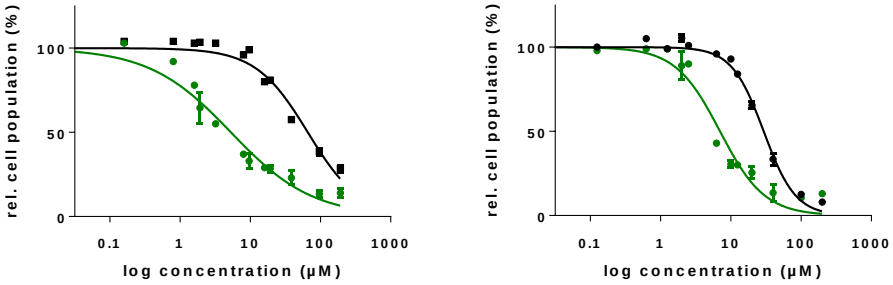

Figure AIV.10. Dose response curves for A549 cells under normoxic conditions treated with [**2**]Cl_2 (left) or [**4**]$(PF_6)_2$ (right) and irradiated with green light (520 nm, 38 J · cm^{-2}) 24 h after treatment (green line) or left in the dark (black line).

AIV.8 Microscopy imaging of A549 cells

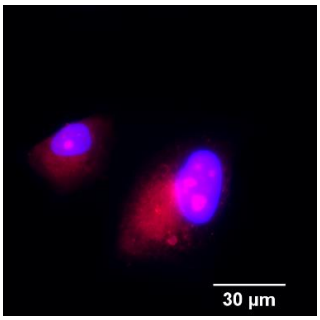

Figure AIV.11. Confocal microscopy imaging of A549 lung cancer cells treated with 25 µM of Azidoplatin and labeled with Rhodamine-alkyne (red) and nuclear stain (Hoechst, blue). The fluorescence mainly accumulates in the nucleoli (merged magenta) of the nucleus, as reported by DeRose and co-workers for HeLA cells.[1]

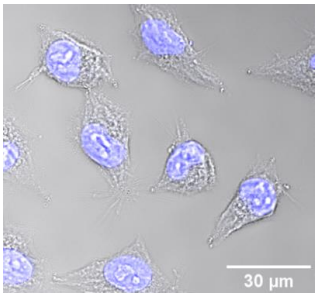

Figure AIV.12. Confocal microscopy imaging of A549 lung cancer cells treated with 25 µM of [**4**](PF$_6$)$_2$ and incubated for 24 h after light irradiation. While the cells look unhealthy, the shape of the nucleus (staining with Hoechst, in blue) is unchanged.

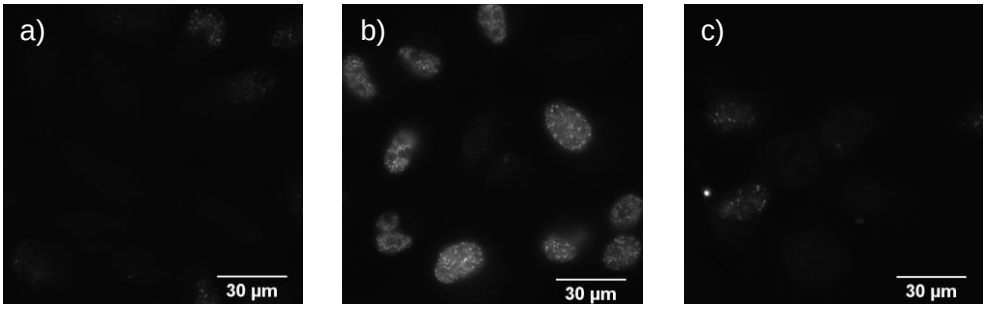

Figure AIV.13. Inverted microscopy imaging of DNA damage co-staining (Phospho-Histone H2A.X (Ser139) Monoclonal Antibody (CR55T33), eBioscience™) in the nucleus of A549 lung cancer cells. Cells are seeded at t = 0 h, treated at t = 24 h, irradiated (517 nm) at t = 48 h, and fixed and co-stained at t = 72 h. a) Untreated cell control, b) cells treated with 10 µM cisplatin, and c) cells treated with 25 µM [**4**](PF$_6$)$_2$. No visible signal in cells treated with [**4**](PF$_6$)$_2$ indicates that the compound does not cause DNA damage.

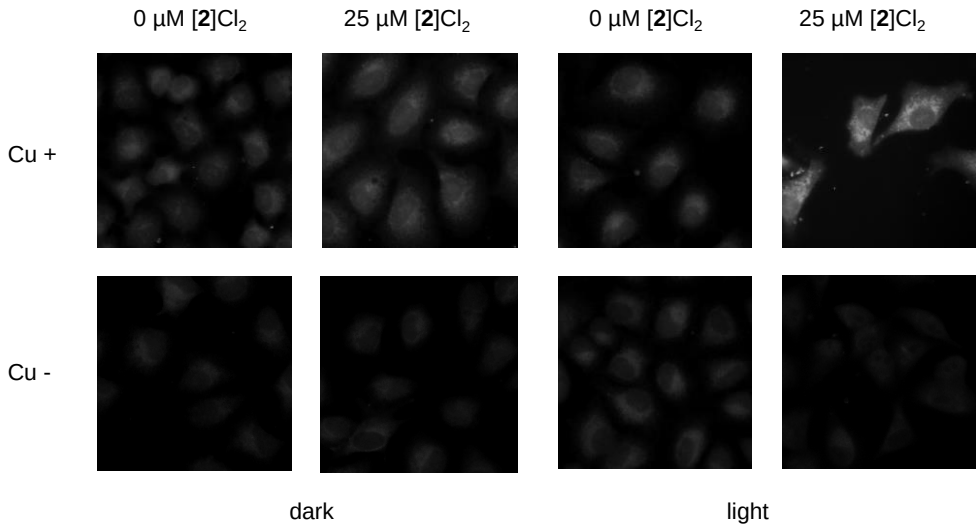

Figure AIV.14. Confocal image of fluorescent labeling of A549 cancer cell lines treated with 0 or 25 µM of [**2**]Cl_2 after fixation, permeabilization, and labeling with Alexa Fluor™ 488 azide, either with or without light activation. Cu-free controls show no fluorescence.

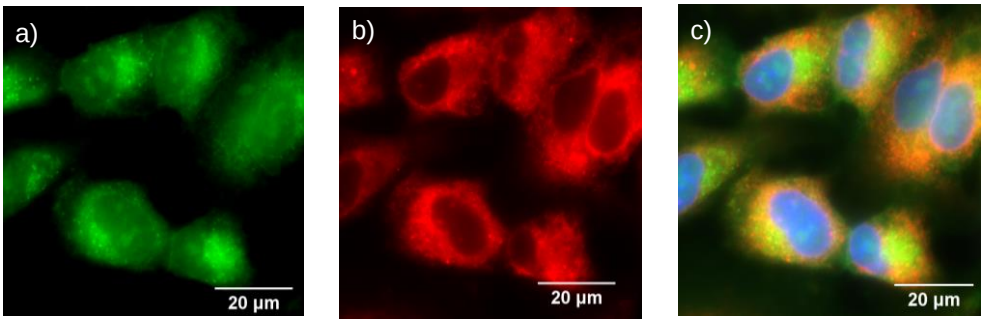

Figure AIV.15. Inverted microscopy imaging of A549 lung cancer cells treated with 25 µM of [**2**]Cl_2 and incubated for 24 h after light irradiation. a) Labeling of [**2**]Cl_2 with AlexaFluor™ 488 azide (green), b) antibody staining (Anti-P4HB antibody [RL90] (ab2792)) for ER with 647 dye (red), and c) overlay of [**2**]Cl_2, ER staining, and nuclear staining (with Hoechst in blue). No co-localization between [**2**]Cl_2 and ER.

AIV.9 DFT studies

Table AIV.2. Nuclear coordinates (Å) of $[\mathbf{2}]^{2+}$ minimized at the DFT/PBE0/TZP/COSMO level in water.

Ru	-0.2371536913409365	-0.04131143665661324	0.3460659281257489
C	-1.532890793872343	-2.602328684055745	-0.8306710061644537
H	-2.251842348881358	-1.911567141887859	-1.252225677621425
C	-1.642526304531791	-3.96624060809431	-1.038131573614926
H	-2.459204774094477	-4.350589289423185	-1.634600041543079
C	-0.7013743566126036	-4.806788840837971	-0.4691272946413964
H	-0.7606423864704916	-5.879266502288916	-0.6057782673450046
C	0.3244371977643025	-4.256496998357359	0.280980597153343
H	1.073834674795002	-4.891602003092336	0.7329816069243424
C	0.3796309229394406	-2.882849869395558	0.452020830275026
C	1.433658431222659	-2.209775445273846	1.229689737130766
C	2.508944179645303	-2.816744716864388	1.854185679326281
H	2.638186424226729	-3.889234316979597	1.828005450072141
C	3.442045979451416	-2.018614854871485	2.521557608428701
C	3.283798981528712	-0.6306698787685715	2.528909377656344
H	4.013082308074423	-0.008006548648022216	3.02708294803903
C	2.188715956496207	-0.07747895341463253	1.888875034334967
C	1.878763640275484	1.357303476414452	1.77341761348179
C	2.678870773488598	2.350340032078643	2.314778091310427
H	3.578432050871337	2.089844977980936	2.855303860191404
C	2.31659698085506	3.677117784872823	2.154734344427466
H	2.932303671824132	4.463886659186145	2.572391886780417
C	1.161037402799495	3.976758199036288	1.453955813852466
H	0.8391700867768646	4.99842639341749	1.301868740976054
C	0.4044605322992431	2.939773235551277	0.9370884192813959
H	-0.5053942363915487	3.133427350325226	0.3837876110025992
N	-0.5561908969102859	-2.061993051065329	-0.09824363547775791
N	1.290643964402534	-0.8729698396351607	1.27972252057514
N	0.7411276968266891	1.656692544693616	1.088450397646056
C	-2.904625694685204	1.30973345151026	-0.4209406170955253
H	-3.159074546272399	1.119331693394778	0.6153244934058034
C	-3.829177188865098	1.972253477042693	-1.246029962462154
C	-5.081237029510736	2.409650093749971	-0.7637294254597728
H	-5.34448276509836	2.229980511678045	0.2726116553637966
C	-5.942831019191246	3.053993630841919	-1.609664473666664
H	-6.905897726169232	3.394462803479109	-1.247638822633878
C	-5.587886540448488	3.281488799698712	-2.957145039524841
H	-6.285976707378517	3.793348696266316	-3.609247377279859
C	-4.378358036899172	2.866462360594738	-3.447234822297753
H	-4.10634271209199	3.042710941226021	-4.48166277226628
C	-3.468728735758551	2.200987135832057	-2.596392809941774
C	-2.203426748938691	1.754980424235831	-3.015489735763675

H	-1.899498739328031	1.931003313573584	-4.038612887354921
C	-1.359976511614206	1.121721902231646	-2.140462249179792
C	-0.01824501729549672	0.6605926787291667	-2.512434950916393
C	0.4817824490667824	0.7264095862799352	-3.787041401434702
H	-0.1230407470131745	1.118646591073996	-4.593612221254457
C	1.783479099821239	0.2780379653931098	-4.071161829436831
C	2.347824843120327	0.3072217645920173	-5.365585833815256
H	1.761832927559798	0.6925704049691234	-6.191994422088704
C	3.622713063068739	-0.1525423362894255	-5.562329286576039
H	4.054548323476805	-0.1323788859786376	-6.556309515466841
C	4.388417037766485	-0.6562377893677332	-4.488377113651005
H	5.394308928850761	-1.014394626269369	-4.672973123771951
C	3.867364508486003	-0.6958141573343313	-3.223514558866063
H	4.446312734937969	-1.082510559177432	-2.392379184937099
C	2.554916147170921	-0.230109285010957	-2.997186517892855
C	1.960413925012303	-0.26628564356595	-1.7255621992893
H	2.526526438672298	-0.6588921698128807	-0.8899822557854268
N	-1.721971209636388	0.8960550899409376	-0.8299180173908062
N	0.7347211632291468	0.1464650390181449	-1.483104476989038
C	-1.845296623246403	-1.922477263098712	2.772395908558176
H	-0.8846884645075135	-2.357346109867444	3.043471661669178
H	-2.280987263610525	-2.460060610957463	1.933930936543366
H	-2.533878589227942	-1.960646866782089	3.613296643274097
S	-1.673802141698928	-0.2010169341142989	2.261105957526909
C	-0.8691121165985981	0.5154409185747081	3.72972950747809
H	0.1926272029382035	0.2662976853549588	3.724018072673569
H	-0.9719533058539879	1.59397919133606	3.600518103505578
C	-1.459294903964237	0.06171005892970272	5.053209670958381
H	-1.217232791103629	-0.9847746283939892	5.235726672069032
H	-0.9774779337303118	0.6479115885820277	5.842142915206382
O	-2.870901701229117	0.1610228170340286	5.131215462211711
H	-3.109650250974828	1.095982201588678	5.115647872970135
C	4.555317496604483	-2.613200219557823	3.179299539713295
C	5.495611468742798	-3.110518769450443	3.738768862794749
H	6.330862662385483	-3.553482201032657	4.23575063131157

Table AIV.3. Nuclear coordinates (Å) of [**4**]$^{2+}$ minimized at the DFT/PBE0/TZP/COSMO level in water.

Ru	-0.1386272406317239	-0.1728871042070829	0.5035144302613997
C	-1.531207832588218	-2.757551541285255	-0.5218677891833204
H	-2.24524195140538	-2.072423656384397	-0.9594936734264196
C	-1.675997338141558	-4.126788522859417	-0.6665537013911703
H	-2.518821125742265	-4.516548561628556	-1.221494992827352
C	-0.7357222835419303	-4.963510374135509	-0.09270650390146704
H	-0.8206172645433322	-6.039053545348915	-0.1819074272165476

C	0.327600867434155	-4.40433911662796	0.5972036675306582
H	1.081112834402843	-5.035730075210719	1.047221963386152
C	0.417181389439417	-3.026298802234863	0.7064797035326705
C	1.523544100393143	-2.343645777494022	1.399681667297997
C	2.60281546127147	-2.953909223144666	2.013882645173779
H	2.693778989773381	-4.030211278213327	2.045507268159674
C	3.586680046685451	-2.153612667407497	2.600332753500335
C	3.467366308803155	-0.7634784683642144	2.545008518012292
H	4.228782042746849	-0.140463455060503	2.991546172989982
C	2.364411606499144	-0.208128963985455	1.920371284871431
C	2.073021538164229	1.227764094915739	1.792468720753408
C	2.913329210355384	2.210394634842851	2.291747916711746
H	3.841052838678216	1.938060530988706	2.775454190403192
C	2.551363903356648	3.540969230760397	2.171238195072737
H	3.197464461409832	4.319428153682459	2.557460879337389
C	1.349901365986842	3.852472938321198	1.559496479888117
H	1.016793496740082	4.876031773882573	1.450620045206895
C	0.5603224057869644	2.825035087576484	1.074174813912468
H	-0.3838218829951246	3.03477308698064	0.5916879604034408
N	-0.5216293835766055	-2.206354272701332	0.155047587701827
N	1.42392386809426	-1.001338278164124	1.379606451031281
N	0.902153017557386	1.537635809657449	1.171604041385557
C	-3.055834875307845	0.4626045292003551	-0.1810695788521076
H	-3.209630041363103	-0.2996710710699634	0.5728062088056303
C	-4.167432105358489	1.128597058235949	-0.7100348312821501
C	-5.487296559209559	0.8327259701647999	-0.295188126423042
H	-5.649178011916466	0.05867265660458093	0.4465769691020724
C	-6.535715999421286	1.52738318379346	-0.8292910015529869
H	-7.549881263621116	1.310463002625711	-0.5151715060764455
C	-6.306593740841212	2.535264578067364	-1.795257130406514
H	-7.15257921015576	3.073712147075788	-2.207278291116568
C	-5.040420298126659	2.839731075786094	-2.214178389097393
H	-4.87024200718328	3.61229575551311	-2.955176724920513
C	-3.935014326520808	2.141688821798193	-1.675169778541516
C	-2.606826972902733	2.373549805060031	-2.057235752150853
H	-2.380759725806299	3.106536976228194	-2.822597109822626
C	-1.583380804479718	1.665282006510563	-1.475154195189084
C	0.6905300303639436	1.006677217215075	-2.179636241328131
C	1.44494098073945	1.188420920758492	-3.313804367195852
H	1.251664988497113	2.043527364600589	-3.950555883023393
C	2.443378017206619	0.2660112487094222	-3.657204325507613
C	3.263160180950746	0.3825685116658833	-4.804067621013719
H	3.141168472402774	1.237076690469951	-5.45994451635968
C	4.196855512988538	-0.5806372607944117	-5.07424441519364
H	4.824449937422036	-0.4888223908618392	-5.953518405341535
C	4.362405104514678	-1.6998334163743	-4.225019509237881

H	5.111492072668192	-2.445424680994455	-4.46387209501423
C	3.582462178063681	-1.841231656677604	-3.112471637118505
H	3.69794148806238	-2.69522755607542	-2.453977974064316
C	2.608949485465777	-0.8600149567651078	-2.811330471509063
C	1.792650759123127	-0.9500685301219021	-1.679588086642163
H	1.914030288175524	-1.799387189712885	-1.020944257503333
N	-1.797857072116594	0.7287145290616694	-0.5059219985511247
N	0.8825410455729213	-0.05063428862247677	-1.341413318084977
C	-0.9111555926772327	-1.705518949397671	3.524696615773443
H	0.1164597094902461	-1.580235719766127	3.861243941079369
H	-1.006703992411256	-2.604271538494385	2.920455738034669
H	-1.585396778980701	-1.785680575273563	4.374319552610008
S	-1.451298510998732	-0.3169425161030515	2.509487491827477
C	-1.105690736513914	1.072592885094073	3.63265678449639
H	-0.03282458910066699	1.265640227898179	3.659755221938439
H	-1.599986077124376	1.928814860253459	3.17030927504548
C	-1.595596377644129	0.8542962781429553	5.05325523832981
H	-0.982706794336715	0.1042891559679136	5.552218599118054
H	-1.457715785829314	1.796290445726972	5.593716128308011
O	-2.93425964451962	0.3989196147537361	5.149703473115839
H	-3.516598099268223	1.102244418313223	4.837021328797476
C	4.704407288681812	-2.748790957023131	3.249952879084972
C	5.64754672222498	-3.246019440854954	3.804782716088554
H	6.486489020537687	-3.687566003023037	4.296774628787286
N	-0.2688007680057821	1.954491933437816	-1.836436878591254
H	-0.2315834179832435	2.747514473869215	-2.461243340831531

AIV.10 References

1 C. Ruppin and P. H. Dixneuf, *Tetrahedron Lett.* **1986**, 27 (52), 6323-6324.

2 R. Wirth, J. D. White, A. D. Moghaddam, A. L. Ginzburg, L. N. Zakharov, M. M. Haley and V. J. DeRose, *J. Am. Chem. Soc.* **2015**, 137 (48), 15169-15175.

APPENDIX V: SUPPORTING INFORMATION FOR CHAPTER 5

AV.1 Synthesis of [Ru(Ph$_2$phen)(mtmp)(RCC-bpy)](PF$_6$)$_2$, [**2a**](PF$_6$)$_2$

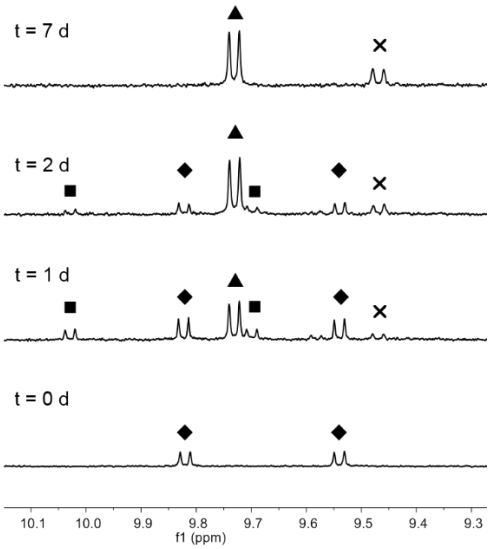

Figure AV.1. ^{1}H NMR evolution during the reaction of [**7**](ClO$_4$)$_2$ and RCC-bpy in methanol-d$_4$ over 7 d at 70 °C. **Key:** ◆ indicates the starting compound [**7**](ClO$_4$)$_2$, ■ indicates an intermediate, ▲ and ✕ indicate the two isomers of 2a.

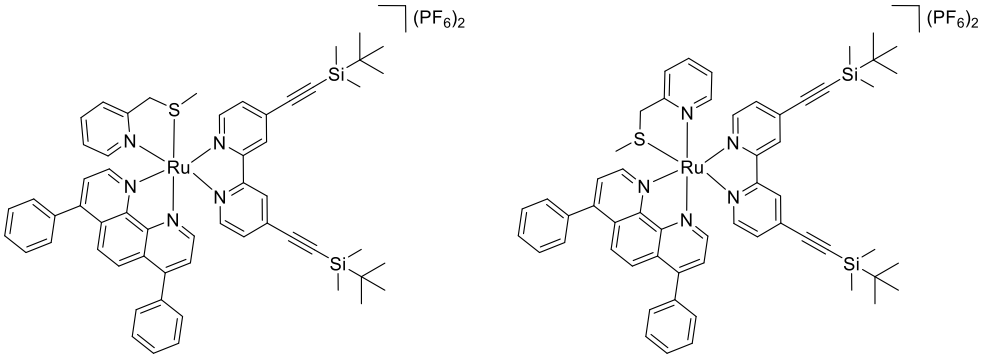

Figure AV.2. The two isomers of [**2a**](PF$_6$)$_2$. Assignment of the two isomers was attempted by 2D NMR NOESY, but was unsuccessful.

AV.2 Stability of RCC-bapbpy over time in solution

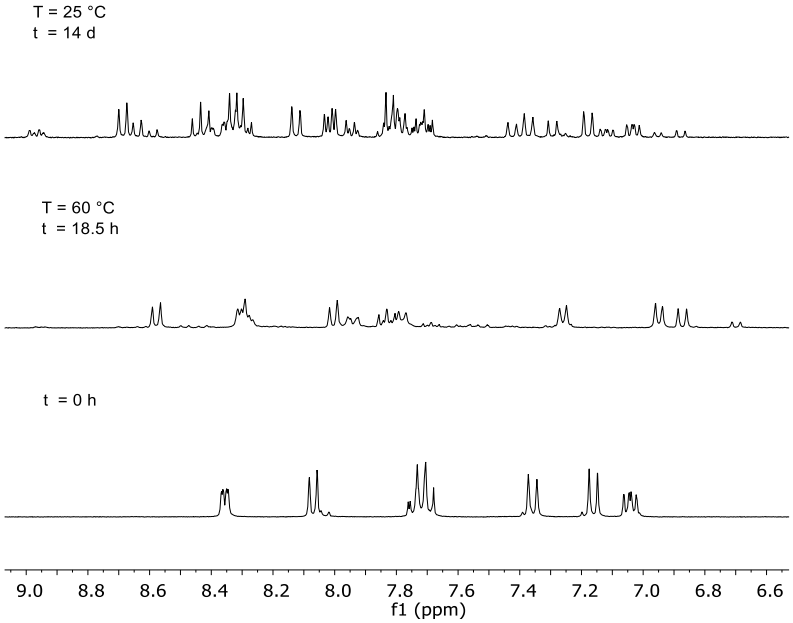

Figure AV.3. ^{1}H NMR spectra of a solution of RCC-bapbpy in ethanol-d_6 over time at room temperature and at 60 °C.

AV.3 Synthesis and rearrangement of HCC-dpa

The reaction procedure was adapted from literature.[1] The reaction was prepared under dry and degassed conditions. Dipyridylamine (0.150 g, 0.880 mmol), tetrabutyl ammonium bromide (TBAB, 0.284 g, 0.880 mmol), and sodium hydroxide (0.176 g, 4.40 mmol) were dissolved in dry dioxane (30 mL), and the reaction mixture was heated to reflux for 1 h while stirring. Thereafter, propargyl bromide (0.1 mL, 0.88 mmol) was added dropwise and the reaction mixture was reacted further for 4 h at reflux. The reaction mixture was cooled down to room temperature, and quenched with 1 M HCl until the pH was below 2. After extraction with pentane (2 times 30 mL), the aqueous layer was basified using solid sodium hydroxide pellets (pH > 12). Then, the product was extracted with dichloromethane (twice 30 mL). evaporation of the solvent yielded the crude product that was purified by column chromatography (silica, dichloromethane/methanol 99/1- 90-10. The pure product was obtained in a yield of 3% (7 mg, 0.033 mmol).

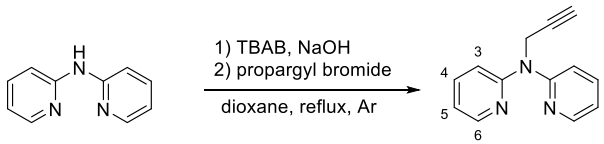

Scheme AV.1. Reaction procedure of the synthesis of HCC-dpa.

^{1}H NMR (300 MHz, chloroform-d, 298 K) δ 8.38 (ddd, *J* = 5.0, 2.0, 0.9 Hz, 2H, 6), 7.55 (ddd, *J* = 8.4, 7.2, 2.0 Hz, 2H, 4), 7.20 (dt, *J* = 8.4, 0.9 Hz, 2H, 3), 6.90 (ddd, *J* = 7.2, 4.9, 1.0 Hz, 2H,5), 4.99 (d, *J* = 2.4 Hz, 2H, N-C$\underline{H}_2$), 2.13 (t, *J* = 2.4 Hz, 1H, CC$\underline{H}$). *^{13}C NMR (75 MHz, chloroform-d, 298 K)* δ 156.3 (2), 148.5 (6), 137.5 (4), 117.7 (5), 114.6 (3), 81.2 (C$\underline{C}$H), 70.5 (C$\underline{C}$H), 37.7 (N-$\underline{C}$H$_2$). *ES MS m/z (calc.):* 210.2 (210.1, [M + H]$^+$).

After several days in solution, new peaks of a decomposition product appeared in the ^{1}H NMR spectrum. The number of these new peaks and integration indicated that the new product is not symmetric. Literature research led to the conclusion that an intramolecular rearrangement took place (Scheme AV.3).[2, 3] In addition, examples where found of the same rearrangement for non-terminal alkynes. A protecting group would therefore not prevent the formation of the new product.

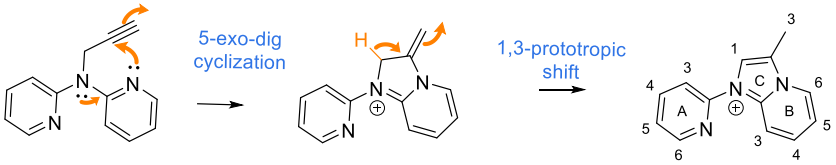

Scheme AV.2. Intramolecular rearrangement of alkyne-functionalized Hdpa ligand.

^{1}H NMR (300 MHz, chloroform-d, 298 K) δ 9.43 (s, 1H, C1), 8.99 (dt, *J* = 9.3, 1.1 Hz, 1H, B3), 8.81 (dt, *J* = 6.8, 1.1 Hz, 1H, B6), 8.58 (ddd, *J* = 4.9, 1.9, 0.8 Hz, 1H, A6), 8.42 (d, *J* = 8.3 Hz, 1H, A3), 8.11 (td, *J* = 8.0, 1.9 Hz, 1H, A4), 8.04 (ddd, *J* = 9.3, 7.1, 1.2 Hz, 1H, B4), 7.68 (td, *J* = 6.9, 1.1 Hz, 1H, B5), 7.44 (ddd, *J* = 7.5, 4.9, 0.8 Hz, 1H, A5), 2.85 (d, *J* = 1.1 Hz, 3H, C3). *^{13}C NMR (75 MHz, chloroform-d, 298 K)* δ 148.7 (A6), 140.9 (A4), 134.9 (B4), 127.3 (B6), 124.2 (A5), 122.2 (C1), 119.2 (B5), 117.2 (A3), 115.3 (B3), 9.5 (C3), all three quaternary peaks are not reported.

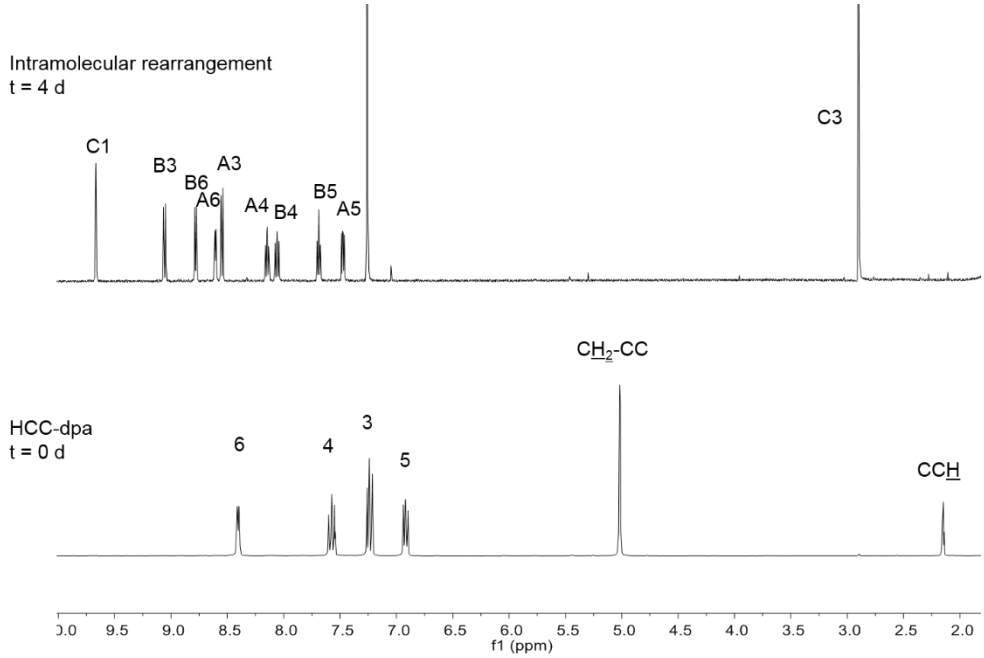

Figure AV.4. ^{1}H NMR spectra of a solution of the alkyne-functionalized HCC-dpa ligand in chloroform-d over time at room temperature.

AV.4 Synthesis and reaction with HCC-bapbpy

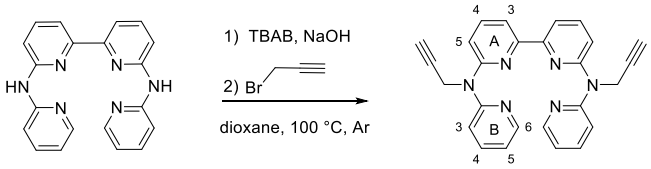

Scheme AV.3. Reaction procedure of the synthesis of HCC-bapbpy.

The reaction was performed under dry, degassed conditions. H_2bapbpy (300 mg, 0.880 mmol, 1 eq), tetrabutyl ammonium bromide (TBAB, 284 mg, 0.880 mmol, 1 eq), and NaOH powder (176 mg, 4.40 mmol, 5 eq) were dissolved in fresh, dry dioxane (40 mL). The reaction mixture was heated up to 100 °C (reflux) and stirred. After 1 h, a solution of propargyl bromide (0.2 mL, 1.76 mmol, 2 eq) was added dropwise *via* a syringe to the reaction mixture. The reaction continued for another 4 h. Then, the reaction mixture was cooled down to room temperature, and quenched with 1 M HCl to decrease the pH below 2. This mixture was extracted with pentane (2 × 60 mL), the aqueous layer was basified using solid sodium hydroxide to pH > 12, and the aqueous layer was extracted twice with dichloromethane (2 × 60 mL). The combined dichloromethane layers were concentrated *in vacuo* to yield the crude product which was purified by column chromatography using silica gel and dichloromethane/methanol (99:1) as eluent. Yield: 110 mg (0.265 mmol, 31%).

^{1}H NMR (300 MHz, DMSO-d_6, 298 K) δ 8.39 (ddd, *J* = 4.9, 2.0, 0.9 Hz, 2H, B6), 7.93 (dd, *J* = 7.6, 0.9 Hz, 2H, A3), 7.84 (t, *J* = 7.9 Hz, 2H, A4), 7.76 (ddd, *J* = 8.4, 7.2, 2.0 Hz, 2H, B4), 7.38 (dt, *J* = 8.4, 0.9 Hz, 2H, B3), 7.29 (dd, *J* = 8.2, 0.9 Hz, 2H, A5), 7.06 (ddd, *J* = 7.3, 4.9, 0.9 Hz, 2H, B5), 5.05 (d, *J* = 2.4 Hz, 4H, N-C$\underline{H}_2$-), 3.06 (t, *J* = 2.3 Hz, 2H, -CC$\underline{H}$). *^{13}C NMR (75 MHz, DMSO-d_6, 298 K)* δ 155.6 + 155.0 + 153.5 (A2 + A6 + B2), 148.0 (B6), 148.8 (A4), 137.9 (B4), 118.1 (B5), 114.8 (B3), 114.2 (A5), 114.0 (A3), 101.3 (-$\underline{C}$CH), 73.2 (-C$\underline{C}$H), 37.1 (N-$\underline{C}$H$_2$-). *ES MS m/z (calc.):* 417.3 (417.2, $[M + H]^+$).

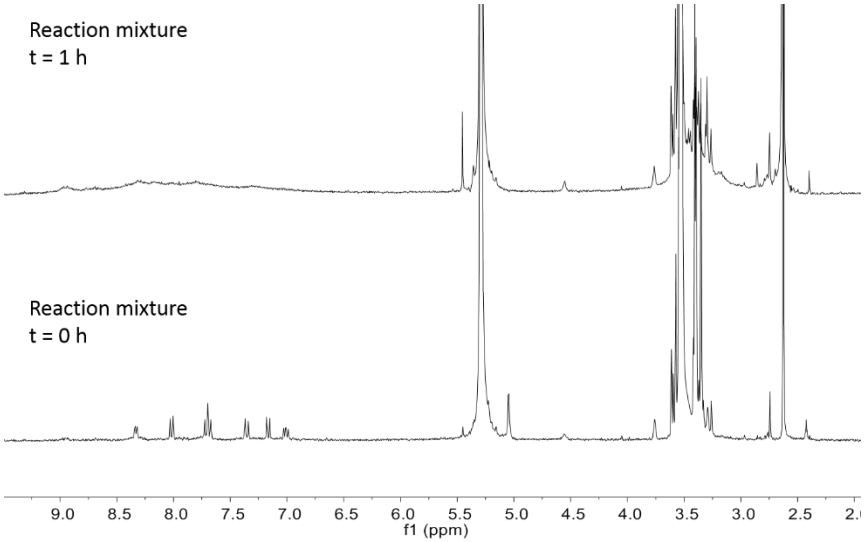

Figure AV.5. ^{1}H NMR evolution during the reaction of $[Ru(DMSO)_4(Cl)_2]$ and HCC-bapbpy in ethanol-d_6 at 60 °C.

AV.5. Enol ester formation on RCC-bapbpy

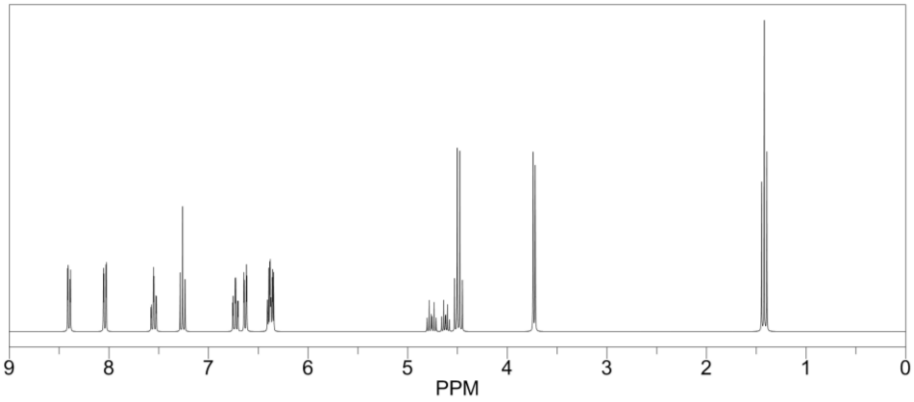

Figure AV.6. Predicted ^{1}H NMR spectrum for enol ester on HCC-bapbpy ligand.

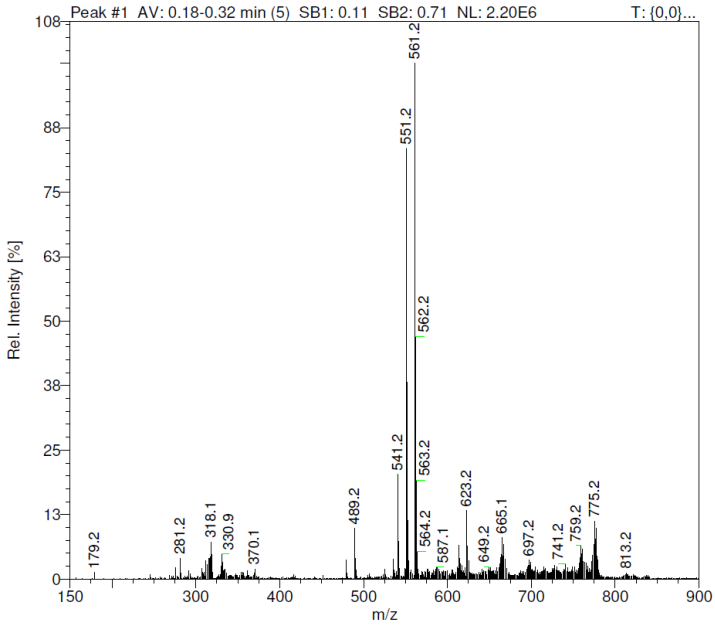

Figure AV.7. MS spectrum of the reaction mixture after reaction of [Ru(DMSO)$_4$(Cl)$_2$] and RCC-bapbpy in ethanol at 60 °C for 18.5 h.

AV.6 References

1 S. Ogawa, N. Kishii, and S. Shiraishi, *J. Chem. Soc., Perkin Trans. 1* **1984**, (0), 2023-2025.

2 M. Chioua, E. Soriano, L. Infantes, M. L. Jimeno, J. Marco-Contelles, and A. Samadi, *Eur. J. Org. Chem.* **2013**, 2013 (1), 35-39.

3 D. Chandra Mohan, S. Nageswara Rao, and S. Adimurthy, *J. Org. Chem.* **2013**, 78 (3), 1266-1272.